THE FEASIBILITY OF PULSE SIGNAL CLASSIFICATION BY SPECTRAL PARAMETERS

John Donald Meloy

NAVAL POSTGRADUATE SCHOOL
Monterey, California

THESIS

THE FEASIBILITY OF PULSE SIGNAL
CLASSIFICATION BY SPECTRAL PARAMETERS

by

John Donald Meloy

Thesis Advisor: S. Jauregui,Jr.

December 1973

The Feasibility of Pulse Signal
Classification by Spectral Parameters

by

John Donald Meloy
Lieutenant, United States Navy
B.S., Purdue University, 1965

Submitted in partial fulfillment of the
requirements for the degree of

ELECTRICAL ENGINEER

from the

NAVAL POSTGRADUATE SCHOOL
December 1973

ABSTRACT

This paper explores the feasibility of fast transform coefficients as classification features for pulse type signals. The fast transforms investigated are Fourier (FFT), Walsh (FWT), and Haar (FHT). A synthesized signal base containing 79 distinct pulse shapes of similar duration is analyzed for classification information compactness in the discrete time, Fourier, Walsh, and Haar bases. Non-parametric information measures are used. It is concluded that a Fourier basis representation enables the significant reduction of dimensionality necessary for further study as a generator of classification features.

TABLE OF CONTENTS

LIST OF TABLES

LIST OF ILLUSTRATIONS

DEFINITION OF SYMBOLS AND TERMS

SYMBOL	DEFINITION
$\underset{\sim}{A}_{MxN}$	A matrix having M rows and N columns.
$\underset{\sim}{A}^T$	The matrix transpose of $\underset{\sim}{A}$.
$\underset{\sim}{S}_k^{(m)}$	The signal space vector representation of the k-th signal of the m-th class.
$s_k^{(m)}(nT)$	The elements of $S_k^{(m)}$ which are samples of the indicated signal taken at time instants nT, n = 0, 1, ..., N-1 and T is the sample interval.
$\hat{s}_k^{(m)}(nT)$	The approximator or estimate of $s_k^{(m)}(nT)$.
$\underset{\sim}{X}_k^{(m)}$	The transform space vector representation of the k-th signal of the m-th class.
$x_{nk}^{(m)}$	The n-th dimensional component or coefficient of $\underset{\sim}{X}_k^{(m)}$.
N	Dimensionality of the space concerned.
M	Cardinality of signal classes in the space.
K_m	Cardinality of signals in the m-th class.
$\hat{\underset{\sim}{\mu}}^{(m)}$	$= \frac{1}{K_m} \sum_{k=1}^{K_m} \underset{\sim}{X}_k^{(m)}$. Estimated mean vector or Prototype for class m.
$\hat{\mu}_n^{(m)}$	The n-th dimensional component of the Protytype.
$\hat{\underset{\sim}{\sigma}}^{2(m)}$	$= \frac{1}{K_m-1} \sum_{k=1}^{K_m} [\underset{\sim}{X}_k^{(m)} - \hat{\underset{\sim}{\mu}}^{(m)}]^2$. Estimated variance vector of class m.

SYMBOL	DEFINITION
$\hat{\sigma}_n^{2(m)}$	The n-th dimensional component of the variance vector of class m.
p_m	The relative current probability that an observed signal should associate with class m.
$\underset{\sim}{\Sigma}$	Covariance matrix.
$\underset{\sim}{C}$	Correlation matrix.
λ_i	The i-th eigenvalue of the real-symmetric matrix $\underset{\sim}{C}$.

TERM	
A/D	Analog to Digital (continuous to discrete) conversion.
FFT	Fast Fourier Transform.
FHT	Fast Haar Transform.
FWT	Fast Walsh Transform.
Global	The whole space, meaning consideration of all dimensions.
Class	The representations of signals from the same source.
Cluster	The collection of points in N-space formed by representations of signal of a common class.

TERM	DEFINITION
Category	The collection of all possible classes to be considered.
Signal Space	The N-dimensional vector space equivalent to the discrete time domain. Its basis is the N-set of block pulses.
Transform Space	The N-dimensional vector space with an orthonormal basis defined by the N transform basis functions.
Feature Space	The $R(\leq N)$ - dimensional vector space formed by discarding selected dimensions of another space.
Coefficient	The projection onto a dimension of the transform space.
Feature	A coefficient selected for use in the classification process.
Metric, or Measure	A function d(a,b) satisfying: 1. $d(a,b) \geq 0$ with equality iff $a = b$, 2. $d(a,b) = d(b,a)$, 3. $d(a,b) + d(b,c) \geq d(a,c)$.
Prototype	The best estimate of the true representation for a class.

ACKNOWLEDGEMENT

I am deeply grateful to ESL, Inc. of Sunnyvale, Calif., for the use of their facilities and the assistance and experience of their personnel. But I am particularly indebted to my wife, Barbara, whose help and unwavering devotion made this work possible and to whom it is dedicated.

I. INTRODUCTION

A. BACKGROUND

Radio-fingerprinting or signal source identification has been regarded with varying degrees of skepticism over the years. Early attempts at radar fingerprinting were based on at most three parameters; signal carrier frequency (RF), pulse repetition frequency (PRF) or interval (PRI), and pulse width (PW). The receivers used for parameter measurements and operator skill differences produced errors great enough to mask subtle differences between individual radars of a type, and often veiled even type identification. The process was of course largely manual, and speed was a function of operator skill and knowledge. And finally, since the data base was compiled mostly from the above observations, the parameter value estimators were not always reliable.

Studies by Stanford Research Institute (SRI) among others, in the early 1960's were influenced by the requirement for greater speed and accuracy and stimulated by advances in computer technology. Advancements in radar such as frequency agility and intra-pulse modulation dictated that measurements of the emitter scan characteristics and modulation type be added to the traditional parameters, RF, PRF, and PW. The emphasis however remained on type classification.

Signal fingerprinting with precision measurement of traditional parameters as the basis as well as some investigation into classification by pulse shape began in the late 1960's. Bennett [1], [2] has explored a number of linear and nonlinear representations of pulse type signals on the basic investigative level. More recent work, as yet unpublished, addresses this problem in an applied manner using linear bases as does the research reported on here.

B. SCOPE OF THE THESIS

The introduction of various fast discrete transform algorithms and the versatile minicomputer has opened new areas in the realm of signal processing and pattern recognition. Although much work has been done on the application of fast transforms, most if it has been in the areas of image processing and two-dimensional character recognition [3], [4]. However, Bennett [1] included two of the three linear bases, and their fast algorithms, (Fourier and Walsh) considered in this research in his work on pulse representation comparison.

The intention of the work reported here is to investigate four orthonormal bases with respect to their suitability in signal source classification using standard pattern recognition techniques. The discrete transforms selected are three of the class possessing fast algorithms, namely, fast Fourier transofrm (FFT), fast Walsh transform (FWT), and fast Haar transform (FHT).

1. Signal Synthesis and Data Base Collection

In order to reduce the number of variables affecting a signal from a set of sources, a data set is synthesized rather than received from actual radars. The result is a set of 79 radar-like pulse trains of high stability and repeatability. Conversion from continuous to discrete form was performed in the laboratory under controlled conditions so that the only noise present in the data base is due to quantization error.

The pulse synthesizer is modeled after the switched, open-line type of pulse forming network found in some early radars. An artificial (lumped element LC) transmission line tapped at each of its 13 section junctions is alternately charged and short circuited by a pulser circuit triggered by a conventional laboratory pulse generator. Fig. 1 contains a schematic diagram of the pulser. By jumpering the section taps two at a time the 79 pulse types were generated.

A large number of pulses of each type (or class) were converted from continuous form to discrete sample values. A wide bandwidth (10 MHz) analog-to-digital (A/D) converter reduced each pulse to a 128 sample, 8-bits per sample representation. The digitized pulse data was then recorded on magnetic tape as the permanent record.

2. Experimental Equipment

All analysis work was performed on the prototype AN/UYQ-9(XN-1) or Parameter Encoder, a general purpose signal analysis computer system composed of a teleprinter, card

reader, graphics terminal, magnetic tape drive, and 1000K word disc file, as well as special purpose A/D and signal processing devices, interfacing with a mini-computer.

Software for this work was specially written for the purpose in Basic Fortran. Included are programs and subroutines to convert (transform) the data on magnetic tape to four 64-dimensional representations, namely, signal or block pulse basis, Fourier, Walsh, and Haar function bases in their discrete forms, and analysis programs which measure the classificatory value of these representations.

Results of the analysis are presented graphically on the terminal cathode ray tube where they are either photographed or processed by a special hard copy unit, or printed by teletypewriter.

3. Theoretic Basis for the Thesis

The question to which an answer is sought in this research is whether any of the rotations defined by the fast Fourier, Walsh, and Haar transforms are useful in a dimensionality reduction sense for the signal data set as prescribed, and is further investigation on more general signal sets and possible application warranted?

The choice of bases is a good mix of properties. Both the Fourier and Walsh bases are global in nature, that is, each coefficient is a function of all coefficients (samples) in the signal. The Walsh and Haar bases are closely related in general shape and by their generating process, while the Haar and signal or block pulse bases have the

common property of being local in nature, that is their functions are nonzero only on a portion of the signal (time) axis.

If it is found that a certain transformation is able to represent the distinctive features of the entire category of signals with relatively few coefficients, then that transform will probably lend itself to an efficient classification process.

To this end the signal data is projected onto the three orthonormal bases and analyzed for classificatory information content and distribution. The methods and measures used are discussed in the context of this research and application.

Although this work stops at feature selection, the only completely valid test for comparison of one set of classification features with another is performance under a specified classification rule. Specifying the rule which best fits the problem at hand is itself sufficient to be the topic of a thesis, and is not considered here. The literature contains both general and specialized studies on the subject of classification.

Two feature selection metrics based on second order statistics are developed and applied to the data. Measures of a potentially more powerful nature such as those founded in information theory are not considered because of the requirement for knowledge of the distributions involved.

A brief discussion of rank order as a feature set is included and could also be the subject of additional work. The use of a ranked vector of feature indices may remove some of the detrimental effects of time reference shift on Walsh and Haar transforms as well as reduce the information to be processed by quantizing the feature space.

4. Results and Conclusions

The signal data base was discovered to contain significant jitter or variation in the time position of the sampling window. The extent and effect of this jitter was not discovered until analysis of the results had begun. Due to time limitation, no attempt was made to reconstruct and reprocess the data.

It is concluded that, in the presence of time jitter, the Fourier basis can result in significant dimensionality reduction, and that the Walsh and Haar bases offer little if any improvement over the signal samples themselves. However, in the absence of jitter an improvement in performance of the Walsh and Haar bases is expected. Considering the speed advantage of the FHT over the FWT and the FWT over the FFT, some compromise to optimality might be indicated for real time processing.

II. EXPERIMENTAL PROCEDURE

A. DATA BASE

Early attempts at the construction of a satisfactory data base were oriented toward reception and digitizing of local radars. This approach, though esthetically satisfying, proved impractical for this work. The data base had to meet several criteria which ruled out the use of "live" signals. First, the objective is to determine the feasibility of fast transform method as generators of high quality classification features, and not to evaluate or specify a complete intercept system for the task. Secondly, there is the "completeness" problem, which is the requirement for the data base to span the range of pulse shapes expected to be encountered. The limited number of radars in the local area limits the completeness of the data. The alternative selected is to employ a pulse synthesizer consisting of a triggered silicon controlled rectifier (SCR) switch driving an open type artificial transmission line pulse forming network similar to those used in early radars [5]. Modern pulse formers are more likely to employ saturable inductances in a high level modulator, but will still produce component value dependent pulse shapes characteristic to that radar.

Figure 1 contains a schematic diagram of the line pulser and its connection to the line and other devices, and also shows the ensemble of pulse shapes which comprise the data

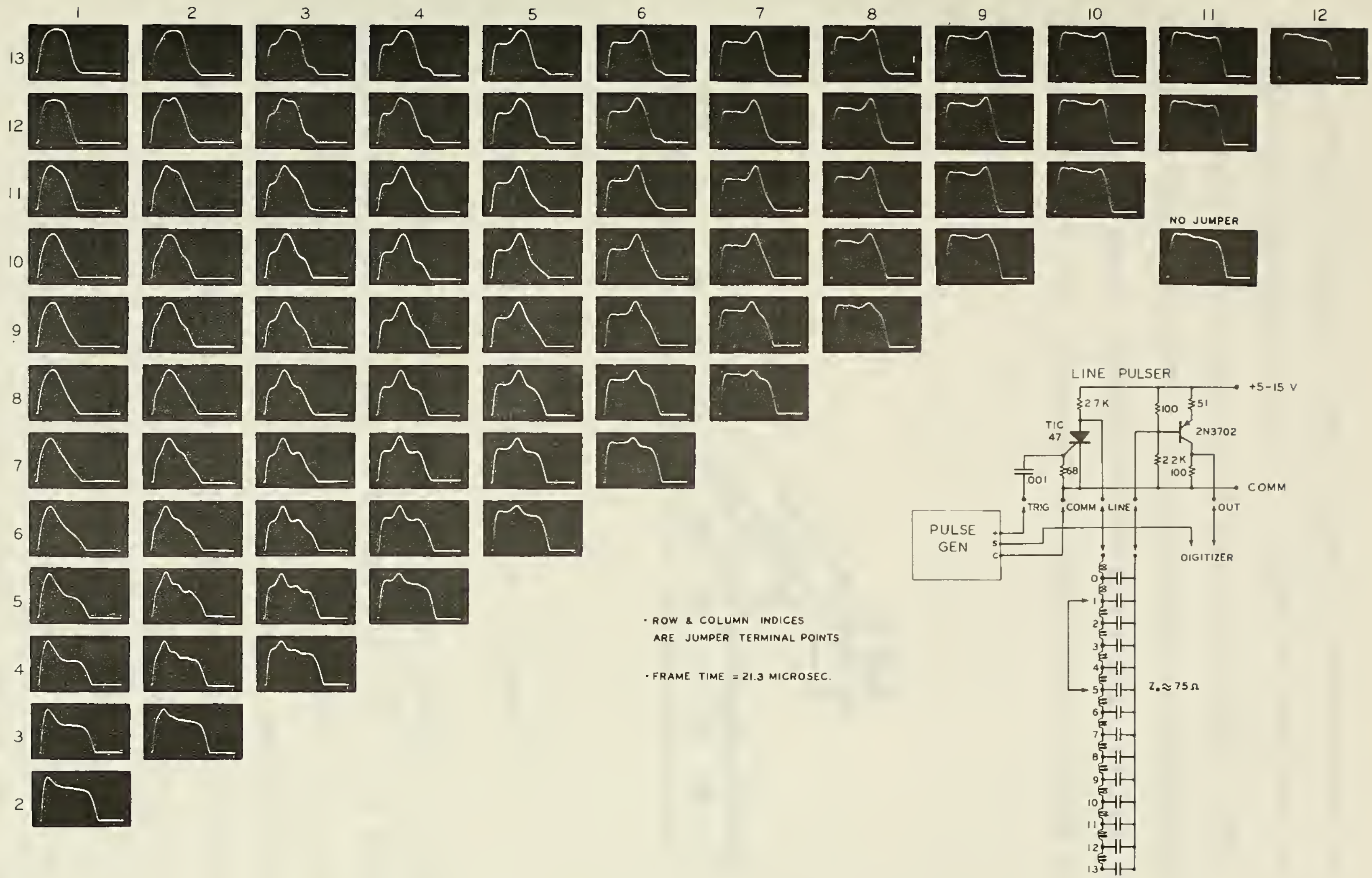

Figure 1. Line Pulser and Pulse Ensemble

base. The artificial line, originally constructed for laboratory experimental use, is tapped at each end and at each LC section junction for a total of 15 taps. The line characteristics and hence the pulse shape are altered by jumpering or short circuiting various taps, creating branches and shortening the length of the main line as shown in Figure 2.

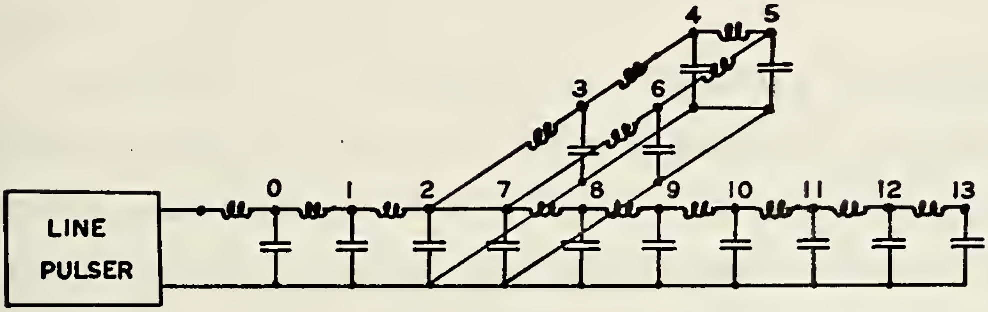

Figure 2. Line Configuration for Class 2-7

In forming the pulse ensemble, 13 taps, number 1 to 13, were exhaustively jumpered two-at-a-time for $\binom{13}{2} = 78$ distinct line perturbations which with the "no jumper" or 1-1 configuration yielded 79 distinct pulse shapes. Referring to Figure 1, note that adjacent pulses are similar both row and column wise, differing mainly in the position and shape of the perturbation. Although they may not accurately represent any given radar's emitted pulse shape, they do span a considerable number of possible shapes for pulses

of similar duration, and are considered a good base for comparison purposes.

The electrical length of the line is 9 microseconds giving a maximum pulse length of 18 microseconds. Observation of all pulse spectra showed that spectral components above 900 KHz are at least 50 db below the largest component. Based on this and a requirement for complete framing of the pulse in a 64-sample window, a sample rate of 3.0 MHz was chosen for digitizing.

Digitizing is the process of converting the continuous voltage waveform output of the line pulser to equally spaced voltage samples converted to 8-bit (256 level quantization) binary numbers or words, and the recording of these samples on magnetic tape. The maximum rate of the A/D converter is 10 MHz, placing the rate used well within device limitations. Each pulse digitization consists of 128 samples, and a total of 4096 pulses for each of two "identical" lines in each of the 79 configurations were committed to magnetic tape, and these make up the permanent data base.

The final step in conditioning the data for analysis is framing of the pulses in windows of 64 samples each. The first sample or the beginning of the window should correspond to a constant amplitude point on the leading edge of the pulse, simulating a threshold crossing triggered sampler. This step is performed manually by placing the joy-stick controlled cursor of the graphics terminal on the desired point of the leading edge of a displayed pulse and commanding

a "store" operation. The algorithm finds and stores the 64 samples following the cursor position in a file on the system's disc. Figure 3. illustrates the flow and form of the data during the data base building process.

It is this last step with its human interaction, and the unsynchronized nature of the digitizing process which are the causes of the window time jitter and the consequently poor data from the non-time-invariant FWT and FHT.

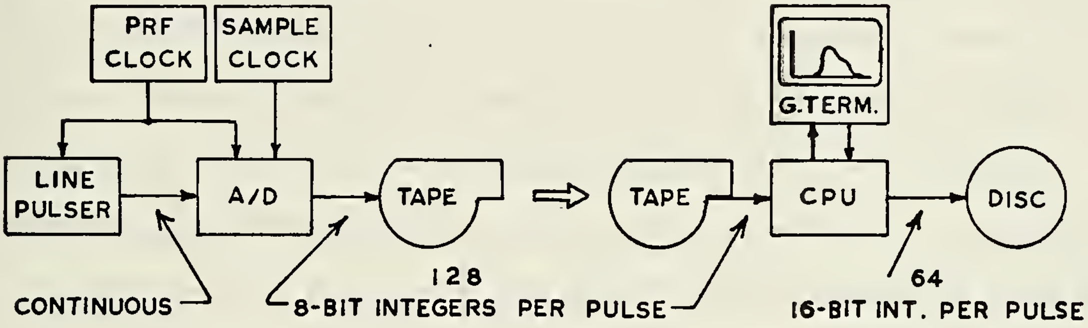

Figure 3. Data Flow and Form During Data Base Construction

B. DATA PROCESSING

The sequency of operations on the signal data base are experimental in nature and are not designed for production type processing although some of the subroutines could be readily adapted for use in an operational program.

Programs written for the Parameter Encoder for this research are listed below with a description of their functions.

1. Program TRED

a. Function

TRED prescreens and transfers the digitized data from magnetic tape to disc file.

b. Description

TRED reads the 128 samples per pulse data from a specified file and record on the magnetic tape, and displays sequentially and individually in graph form on the terminal CRT those pulses which exceed a preset threshold value. If the signal is noisy, that is, contains parity errors or is not of the desired type due to an error in jumpering the pulsed line, it can be rejected. If the data is suitable for further processing, the operator places the cursor crosshairs at the leading edge of the pulse. The 64 samples following the leading edge are stored on the disk as 64 16-bit integers. The program may be terminated at any time.

2. Program SIFT

a. Function

SIFT calls those signals stored by TRED and performs 1, 2, or 3 fast transformations on the data. The transform coefficients are then stored along with the signal data in a separate class structure file on the disc.

b. Description

SIFT can optionally perform a second screening of the data enabling cursor positioning errors to be detected, or it may automatically and sequentially process any signal data located in TRED's file. The three transformation which can be performed are subroutines and are easily changed. All transform coefficients are normalized to the average value (zero-th order coefficient) and then stored as 64 floating point numbers in a disc file location in space set aside for that particular pulse type or class. Listings of the fast transform subroutines are provided in Appendix C.

3. Program MEVAR

a. Function

MEVAR calculates the class mean and variance.

b. Description

MEVAR uses the transform data stored by program SIFT to calculate the mean values of each coefficient of each transform for the signal type or class specified. The means are stored and then used to calculate the variance or second central moment of each coefficient and transform. These class data are stored in a third disc file.

4. Program GVAR

a. Function

GVAR is a feature selector program calculating a measure of feature goodness based on the average fluctuation of class mean values weighted inversely to class variation.

b. Description

GVAR uses the class data of program MEVAR to calculate a global central second moment from weighted class data. The results are presented in original coefficient and also in ranked order.

5. Program FRAT

a. Function

FRAT is a feature selector program similar to GVAR. The measure of goodness it employs includes a weight which is a function of the number of members in each class. The results can be interpreted as a kind of signal to noise ratio where the signal is classificatory information and noise is the average within class variance of the signal transform coefficients for each dimension.

b. Description

FRAT uses the class average data of program MEVAR as does GVAR. The results are presented in original coefficient order and in rank order.

III. SIGNAL TO TRANSFORM SPACE - PROJECTION

A. TRANSFORMATIONS AND CLASSIFICATION

At this point the terminology and notation employed for the remainder of the thesis will be standardized and oriented toward linear vector spaces and the classification problem rather than to physical concepts.

The question "why transform?" may be asked with some validity. Any operation on a signal requires time and expense. The answer, fundamental to the field of pattern recognition, is reduction of dimensionality. A complete description of any possible signal representable in a space of dimension N requires all N dimensions. For signals emitted by a specific source, the N-dimensional representations will be similar and will differ in some manner from representations of signals from another source. The problem of classification is how to measure this difference so that classification errors are somehow minimized. If all N dimensional projections contain significant information then all N must be included in the metric. However, if this signal space can be rotated somehow so that the information in some of its dimensions can be projected onto a single dimension in another space, then the information has been compressed or dimensionality reduced. However, a rotation that works for one signal class probably won't work for all signal classes in the category of signals of interest. The criteria

and evaluation methods for a transformation are discussed in Section IV.

B. THE FAST TRANSFORMS

The primary reason for selection of the Fourier, Walsh, and Haar discrete transformations is the existence of fast algorithms based on elimination of redundancy [3], [4], by matrix factorization of the basis matrix. An N-dimensional transformation in general requires N^2 real or complex multiplications. A FFT or FWT requires but $N\log_2 N$ arithmetic operations (complex multiplications for the FFT and real additions for the FWT). A FHT because of its highly local nature (lots of zeros in the transform matrix), requires only 2(N-1) real additions and N-2 normalizing multiplications.

Another important reason for the selection of discrete Fourier, Walsh and Haar transforms is the difference in the basis functions of the transformations. Appendix B addresses the Walsh/Hadamard and Haar functions in greater detail. The Fourier and Walsh functions possess similarities such as the average number of sign changes per unit interval and even/odd symmetry which lead to the terms sequency, sal, and cal for the Walsh functions. Furthermore, the Walsh and Haar functions are closely related.

A final comment on the translational invariance is in order. The Fourier basis representation is invariant under time translation while the Walsh basis is invariant under dyadic translation. That is, the Fourier magnitude coefficients do not change when the signal data samples are

cyclically translated, that is,

$$S_1 = (S_0, S_1, \ldots, S_{N-1})$$

$$S_2 = (S_{(0 \oplus k)}, S_{(1 \oplus k)}, \ldots, S_{(N-1 \oplus k)})$$

where $\oplus$ indicates modulo(N) addition. This is equivalent to sliding the signal in the reference frame. Walsh coefficients do change under this type of translation but are invariant when signal data are translated or reorder according to the mod(2) bit-by-bit sum of the original index and the translation constant, k.

$$S_1 = (S_{\ldots 000}, S_{\ldots 001}, \ldots, S_{1\ldots 11})$$

$$S_2 = (S_{(\ldots 000 \oplus k)}, S_{(\ldots 001 \oplus k)}, \ldots, S_{(1\ldots 11 \oplus k)})$$

where $\oplus$ now indicates modulo(2) bit-by-bit addition and k is an integer expressed in binary form. For this application, dyadic invariance is not beneficial, but if time translation is minimized this drawback is not serious. The Haar transform is also not time invariant.

Figures 4, 5, 6, and 7 are plots of the 64 dimensional representations of the data for the 79 pulse classes 1-2, 1-3, 1-4, ..., 11-12, 11-13, 12-13. Referring to Figure 1, the class sequence progresses up the columns moving from left to right. The spaces are signal, Fourier (magnitude), Walsh, and Haar in Figs. 4, 5, 6, and 7 respectively.

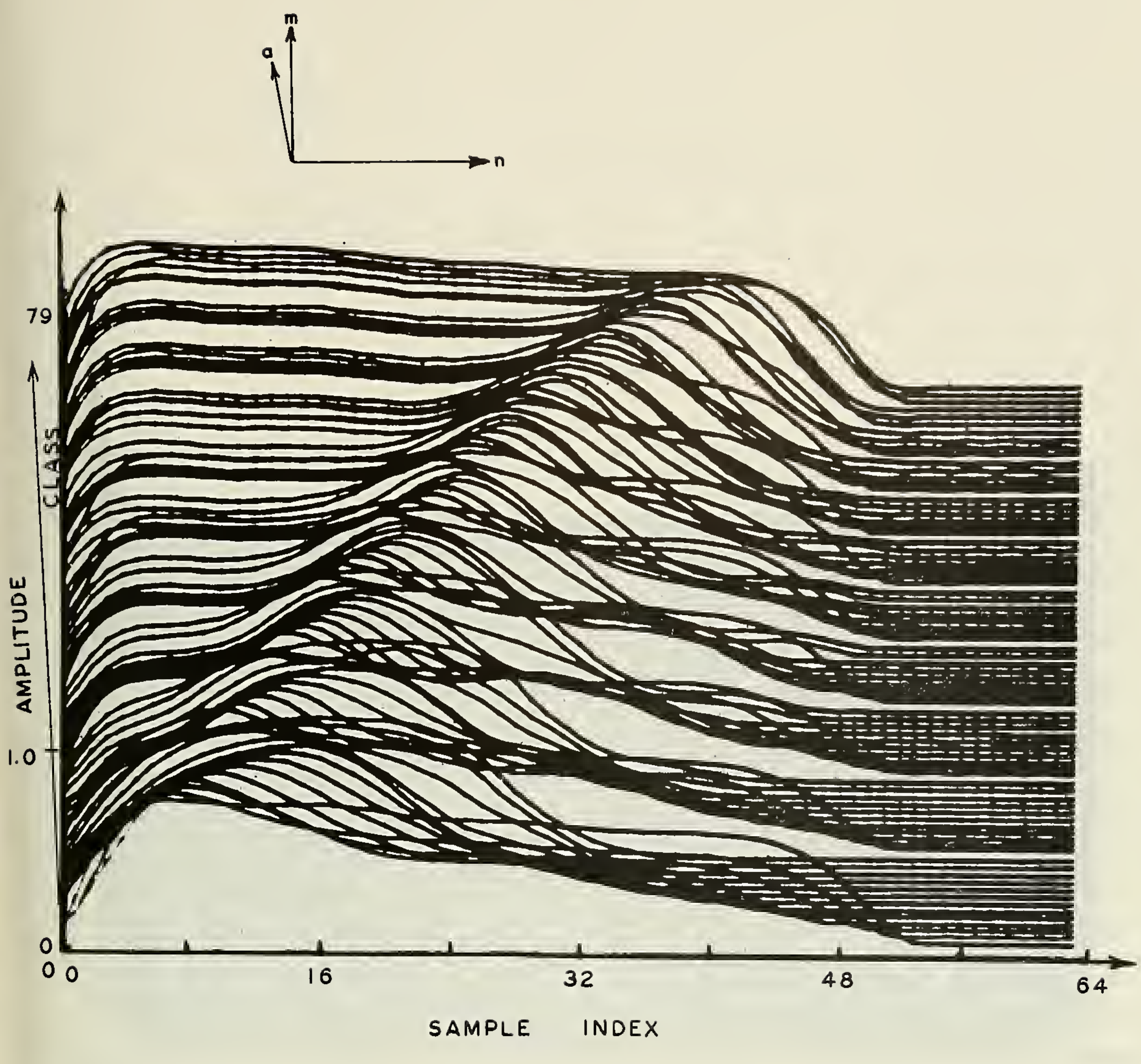

Figure 4. 3-Axis Plot of Prototype Signals of the 79 Classes

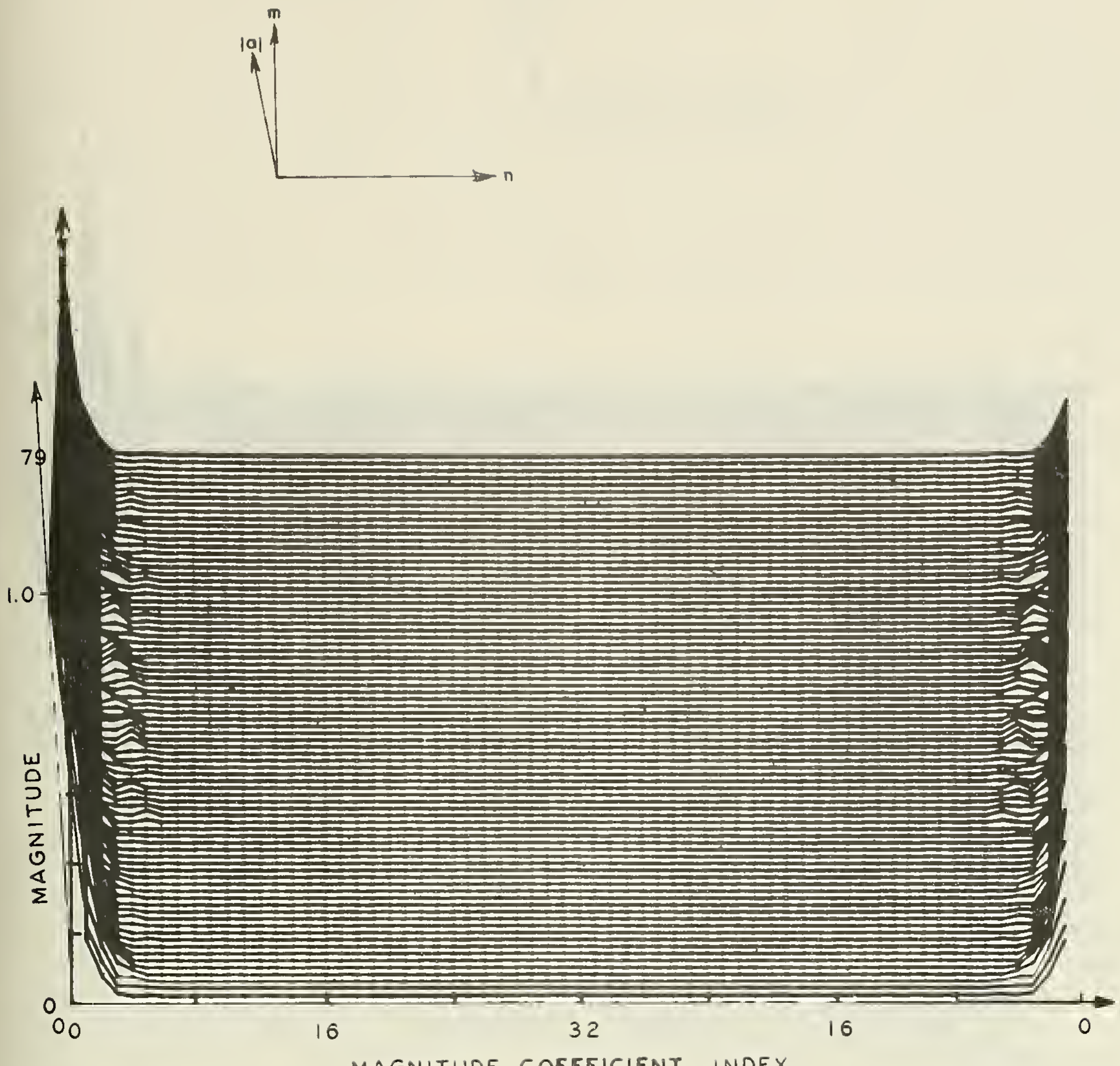

Figure 5. 3-Axis Plot of the Fourier Prototypes of the 79 Classes

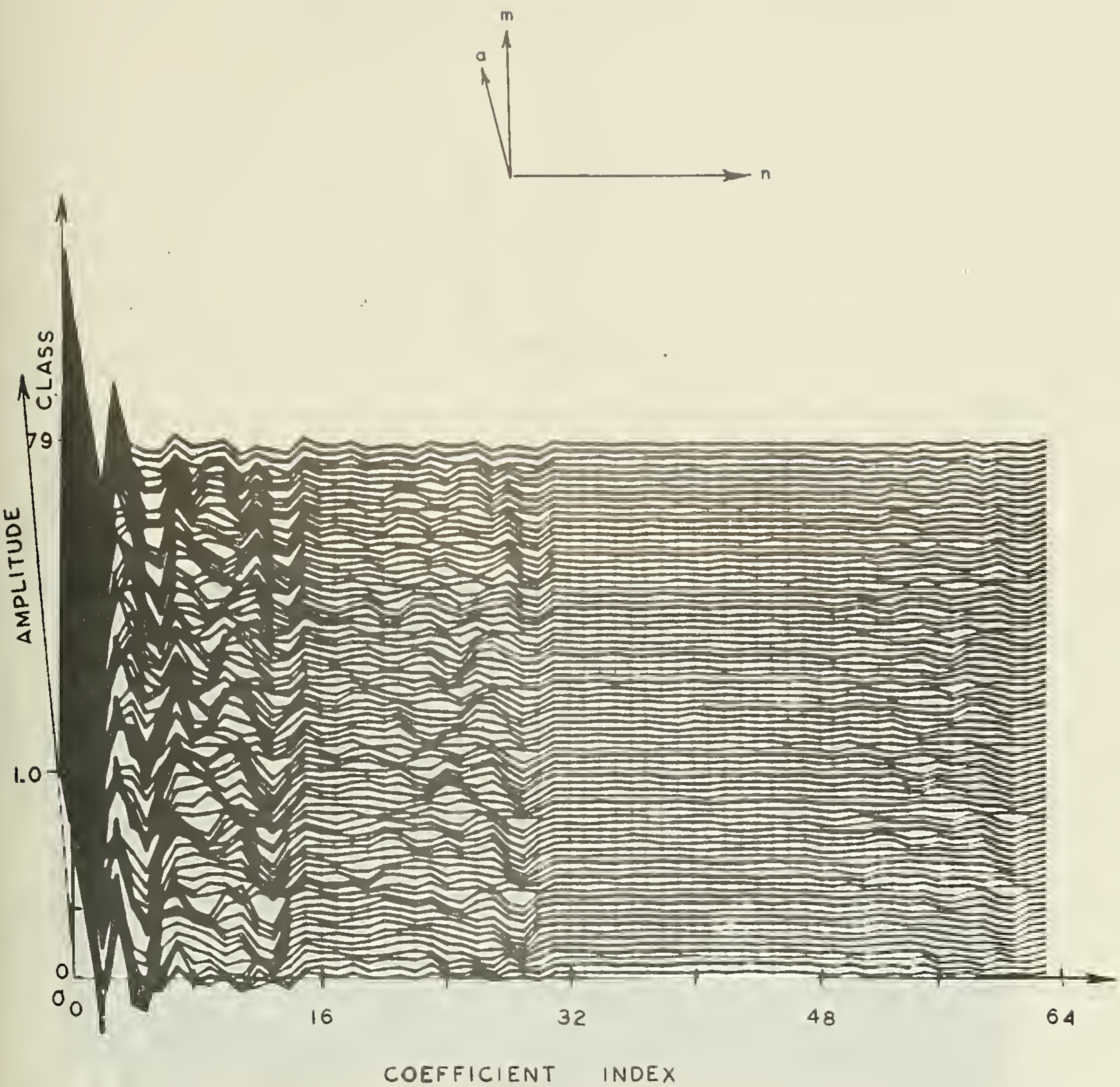

Figure 6. 3-Axis Plot of the Walsh Prototypes of the 79 Classes

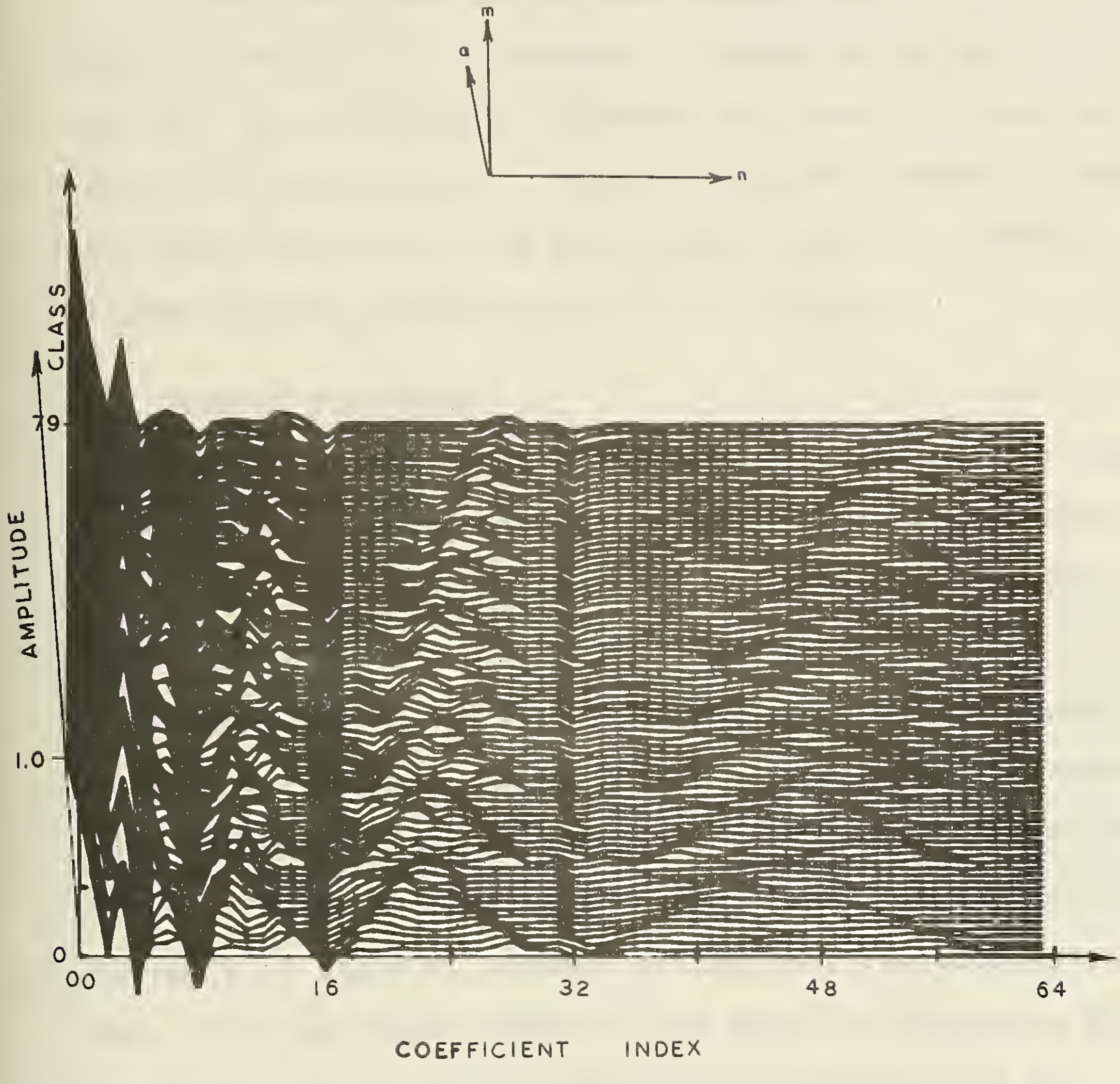

Figure 7. 3-Axis Plot of the Haar Prototypes of the 79 Classes

IV. DIMENSIONALITY REDUCTION - FEATURE SELECTION

A. PURPOSE

A main principle in pattern recognition is the elimination of redundancy and useless information in the given data so that the classifying algorithm can make efficient use of both time and machines. This elimination process is dimensionality reduction, and the process itself is commonly termed feature selection [3], [4], [7]-[9].

B. FEATURE SELECTION

The projection of an N-dimensional signal vector representing an N-sampled time function from the signal space to a transform space by means of a complete orthonormal transformation does not in any way inherently reduce the dimensionality of the representation. However, a transformation of this type can be viewed as measuring the correlation between the signal and each of the N basis functions. Hence it seems reasonable to assume that, given a certain category of signals, certain orthonormal transformations are more efficient than others in the sense of requiring fewer coefficients to attain whatever the objective may be.

If the objective happens to be representation of the signal in more compact form, then perhaps all transform coefficients smaller than some threshold value could be eliminated, resulting in a reduction from N to, say, K dimensions. Then the representation obtained from the

inverse transformation back into the signal space is the best S_k approximator of the original signal in terms of that orthonormal basis. See Appendix A. The "closeness" of this approximate representation is commonly measured in terms of mean square (or energy) error (MSE), which in vector space context is the squared Euclidean distance. This error is given by

$$MSE = \frac{1}{N} \sum_{n=0}^{N-1} (s(nT) - \hat{s}(nT))^2$$

where: $s(iT)$ are the original signal samples

$\hat{s}(iT)$ are the signal approximator "samples"

T is the sample interval.

For the purpose of classification of signals the elimination criteria are different, and the MSE of the before and after representations is not necessarily a good measure. Some of the most distinctive characteristics of a signal may contain very little energy. Their elimination causes little energy error but a large loss of classificatory information in the reduced representation.

Consider the signals $s_i(nT)$, $n = 0, 1, 2, \ldots, N-1$, $i = 1,2,\ldots,I$ originating from $M \leq I$ source classes all from the category of interest (pulsed signals from different sources of the same type). The N-dimensional vectors formed by the signal samples define I points in the transform space which will tend in some manner to form M clusters

representing the M source classes. For a given orthonormal transformation the I points will project onto each of the N basis vectors and clustering to some extent will occur in each dimension. The dimensional cluster for, say, class m_1 will exhibit some spreading which is related to the manner in which signal perturbations and system noise project onto that particular basis vector. Another class, m_2, will similarly cluster on that dimension with some spreading. The difference between the cluster mean values is a measure of that dimension's classificatory information, the use of which in classification is degenerated by the intra-class spreading.

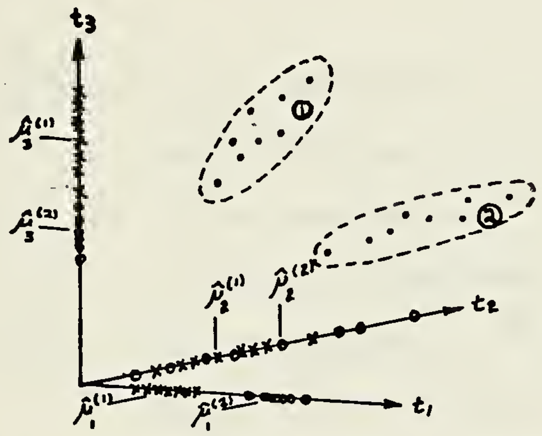

Figure 8. Hypothetical 2-Class Projection onto 3 Orthogonal Axes.

Figure 8 is a 3-dimensional, 2-class hypothetical example. The projections of both classes m_1 and m_2 on basis axes t_1 and t_3 exhibit small spreading, however the cluster separability on axis t_1 is clearly greater than on axis t_3. The

projections onto axis t_2 are widely spread and even though the mean values differ considerably, no separability exists.

This illustration suggests a class of feature selection metrics based on the concept of signal (information) to noise ratio. The two feature selection metrics investigated in this thesis are both of this type. The first is simple and intuitive, used primarily for purposes of illustration. This metric is incorporated in Program GVAR and can be expressed as

$$G_n = \frac{1}{M-1} \sum_{m=1}^{M} \frac{(\hat{\mu}_n^{(m)} - \hat{\mu}_n)^2}{\hat{\sigma}_n^{2(m)}}$$

where:

$\hat{\mu}_n^{(m)}$	is the estimated n th dimensional mean for class m,
$\hat{\mu}_n$	is the estimated n^{th} dimensional average of class mean estimates,
$\hat{\sigma}_n^{2(m)}$	is the estimated n^{th} dimensional variance for class m, and
M	is the number of classes in the category.

There is no compensation for differences in cardinality of class populations, and it is sensitive to round-off errors encountered when the dimensional projection means and the variances are nearly equal and very small as would occur if the basis vector for that dimension were orthogonal to

everything in the signal vector. This instance occurred in the case of the Haar basis, some functions of which are non-zero only in regions where the signal is either zero or a constant.

This test is simply the average of the ratios of squared class mean deviations from the global average to class variance. Because of the sensitivity to computational errors, the results may be misleading. It does lead naturally to a more powerful and less sensitive variance ratio test incorporated in Program FRAT.

This latter test is a modified form of the Snedecor F test so called for Fisher on whose Z distribution the test is based [10]. Snedecor's F test as used here provides, in addition to a relative goodness number, a confidence percentage that the variance among class mean values is not due to the average intra-class variance (or noise). However, it is modified slightly to reflect the relative probabilities of occurrence of a class. The metric F is given by

$$F_n = \frac{\frac{1}{M-1} \sum_{m=1}^{M} p_m (\hat{\mu}_n^{(m)} - \hat{\mu}_n)^2}{\frac{1}{M} \sum_{m=1}^{M} p_n \sigma_n^{2(m)}}$$

$$= \frac{\frac{1}{M-1} \sum_{m=1}^{M} K_m (\hat{\mu}_n^{(m)} - \hat{\mu}_n)^2 / \sum_{m=1}^{M} K_m}{\frac{1}{M} \sum_{m=1}^{M} K_m \sigma_n^{2(m)} / \sum_{m=1}^{M} K_m}$$

where:

p_m is the relative probability of occurance of class m (more properly that an observed signal came from source class m), and

K_m is the number of signals in class m.

A comparison of the results of the G test and the F ratio test indicate that the latter is not as sensitive to data and computational problems.

Signal-to-noise or variance ratio type tests are not the only metrics for feature selection. Several information theoretic approaches have been applied to multiclass classification [7], [8]. There are other, perhaps more elegant methods, applicable to the two class problem or the clustering problem [9].

From the feature selector algorithm results a subset of coefficients is chosen which can be tested further for optimality. Of course the only valid test is minimization of classification error, a test not performed here because of time limitations.

C. COVARIANCE AND CORRELATION

While feature selection tests will in general measure the classificatory information a feature (or dimensional projection) contains, they are not sensitive to the kind of information but rather only to the average net accumulation.

If the pulse signal classes of concern have hypothetical linearly independent details, say A, B, C, and D, which occur

in various linear combinations to characterize the classes, then the optimal linear orthogonal transformation which can be performed on the signal data is the one which is able to project each detail onto its own dimensions. Restated, let the basis vectors of the transformation be generated from the signal details so that the projections in the transform space are mutually uncorrelated. Sebestyen [9] proves that this transformation (followed by a diagonal feature weighting transformation) is the optimum linear transformation for feature generation. This transformation is variously called Holelling's Method of Principal Components, Karhunen Loeve Transform, and factor analysis. The matrix defining the transformation is the matrix Σ_S of the signal set.

$$\underset{\sim}{P}^T \underset{\sim}{\Sigma} \underset{\sim}{P} = \text{diag}(\lambda_o, \lambda_1, \ldots, \lambda_{N-1})$$

where the λ_i are the eigenvalues of Σ_S, and

$$\lambda_o \geq \lambda_1 \geq \cdots \geq \lambda_{N-2} \geq \lambda_{N-1}.$$

P is the matrix of eigenvectors corresponding to the eigenvalues, λ_i.

While this transformation would appear to be the solution to the problem, there are aspects of pulse source classification which nullify its attributes. Most important is the fact that it is a complete orthogonal transformation only for the signal from which it was generated. New features

of new signal source classes will be undetected unless they contain a linear combination of one or more of the transform basis vectors. Secondly, since the basis is data dependent and not composed of a fixed set of orthonormal vectors, no factorization and hence no fast algorithms are possible. This means that the transformation will require N^2 real multiplication operations and that unless the feature space can be greatly reduced, an application where speed is important cannot use it.

The covariance matrix Σ_T is calculated for the reduced feature sets derived from the three fast transforms investigated. These are presented in the next section in normalized form as correlation matrices. Ideally, feature vectors of all signals in all classes, i.e., all observations, should be used in the calculation of a global correlation matrix; however, due to machine limitations, only the class mean feature values were used since they are the best statistical estimate of actual feature values. The covariance matrix is then:

$$\Sigma_T = [\hat{\mu}_n^{(m)}]_{N x M}^T \; [\hat{\mu}_n^{(m)}]_{M x N}$$

$$= [(\hat{\mu}_i^{(k)} \; \hat{\mu}_j^{(\ell)})]_{N x N}$$

where i,j range over 1, 2, ..., N independently and k,ℓ range over 1, 2, ..., M independently.

The correlation matrix is obtained by normalizing all elements to the inverse square roots of the diagonal elements which are the global variances of the class means.

$$\underset{\sim}{C}_T = \left[\frac{\hat{\mu}_i^{(k)} \ \hat{\mu}_j^{(\ell)}}{(\hat{\mu}_i^{(k)})^2 \ \ (\hat{\mu}_j^{(\ell)})^2} \right]_{N\times N}$$

where i, j, k, ℓ, are as defined above.

Off diagonal elements C_{ij} reflect the degree of correlation between features of index i and j.

D. RANK ORDERING

To this point only continuous measures in continuous vector spaces have been considered. It is possible that a discrete space might be entirely suitable if not superior when the inter-class distances and intra-class variances under a discrete metric are such that a quantized space does not increase classification error.

Consider the case of ordering the features, selected for their information content and derived from a complete orthonormal transformation of the signal space as above, in decreasing value order. If the reordered feature indices rather than the feature values are used for classification, the information rate between the signal processing device and the classifier could be reduced considerably. The classifier itself could possibly be simplified.

Using the data of this thesis for example, data samples are 8-bit integers and the projections in the transform

space are floating point numbers requiring 32-bits. If the number of features used for classification is 16, then, for each pulse observation 512 bits must be sent to and processed by the classifier. Now if only the rank orders is preserved, the 16 features are represented as 4-bit integers and each pulse observation results in transmission and processing of 64-bits. For a given channel bandwidth, significantly more information could be sent per unit of time if a suitable classifer can be found.

The feature space becomes quantized with N! = N(N-1)(N-2) ...(2)(1) distinct points corresponding to all different possible orderings of N features. For the case N = 16 there are more than 2 x 10^{13} distinct points. The 3-feature space is illustrated below.

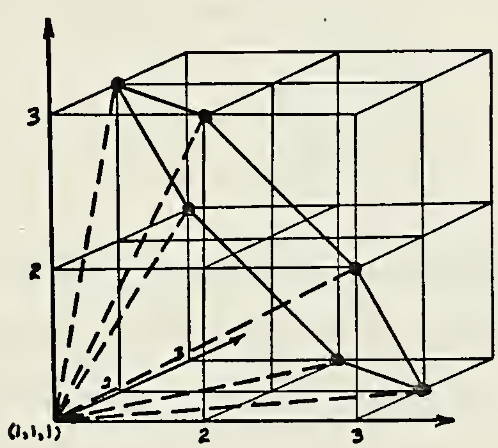

Figure 9. 3-Space Representation of all Rank Ordered 3-Vectors (I_1, I_2, I_3)

There are tests which can be applied to ranked sets which could find application to this problem. Moroney [10] discusses several in the context of evaluating judges asked to rank things in order of quality. A test which evaluates the degree of agreement within a group of rankings (a class cluster) compares the mean squared difference of perfect agreement ranking and the expected ranking. The expected ranking is the average of all possible rankings and is indeed not a ranking at all, but an N-vector with all entries equal to N(N+1)/2. The result is a number between 0 and 1 called the Coefficient of Concordance by Moroney. This test might find use as a feature evaluator since it provides a measure of intra-class fluctuation.

Another test measures the correlation between two rankings and yields a number, R, between -1 and +1 given by the empirical appearing formula

$$R = 1 - \frac{6 \sum_{n=1}^{N} d_n^2}{N(N^2 - 1)}$$

where d_n is the difference between ranked indices. R is called Spearman's Rank Correlation Coefficient and might be employed in classification, measuring the correlation between an unknown ranking and the mean ranking of classes taken one-at-a-time.

Rank ordering was not considered in this investigation, but it appears to warrant further study.

V. DISCUSSION OF RESULTS AND CONCLUSIONS

The intention of this research is to explore the feasibility for generating classification features for pulsed signals by linear transformation using so-called fast algorithms. The underlying premise is that the pulse generation mechanisms of distinct sources impart sufficient information to the pulse (envelope) shape to allow classification on this basis. A complete orthonormal transformation process cannot create information, and, by the completeness property, does not destroy it. The hypothesis is that such a transformation will result in a more efficient distribution of classificatory information than is inherent in the signal. Restated, the pulse shape representation in signal space requires consideration of more dimensions for a specified classification confidence level than does some transform space defined by a fast discrete method.

In Section IV it was stated that the Karhunen-Loeve transform is optimal for a closed, invariant set of features, and results in the least dimensionality for a specified error tolerance under a MSE metric. It does not, however, meet the fast algorithm requirement. Thus it is sought to determine if the FFT, FWT, or FHT results in a compacting of classificatory information significant enough to warrant further investigation and possibly application.

The discrete representation results in a dimensionality of 64 for the signal space and each of the transform spaces.

Using the second order statistics of the 79 signal classes, and treating the projection onto each dimension as a classification feature, two measures of information content were applied to each of the transform spaces. The F Ratio metric was then applied to a subset of 20 signal classes to provide a comparison between the three transform spaces and the signal space to substantiate the hypothesis that a transformation (or rotation of the space) can result in a more compact representation for classification purposes.

A. INTERPRETATION OF DATA

A complete listing of numeric data is presented in Appendix D.

A comparison of the transform class prototypes, that is, the class estimated centroid in N-space, is shown graphically in Figures 10, 11, 12, and 13 for signal, Fourier, Walsh, and Haar representations. These figures consist of 79 superimposed curves consisting of lines connecting data points which are signal samples for Fig. 10 and transform coefficients for Figs. 11 to 13. The data are scaled differently for illustration purposes.

The collection of points of intersection of the overlaid curves and a line drawn vertically from any index point, n, gives one an indication of the distribution of the class mean values, $\hat{\mu}_n^{(m)}$ on the n^{th} dimension.

Figures 14, 15, and 16 are graphs illustrating the measure of classificatory information and its distribution. The horizontal axis is calibrated by index of decreasing

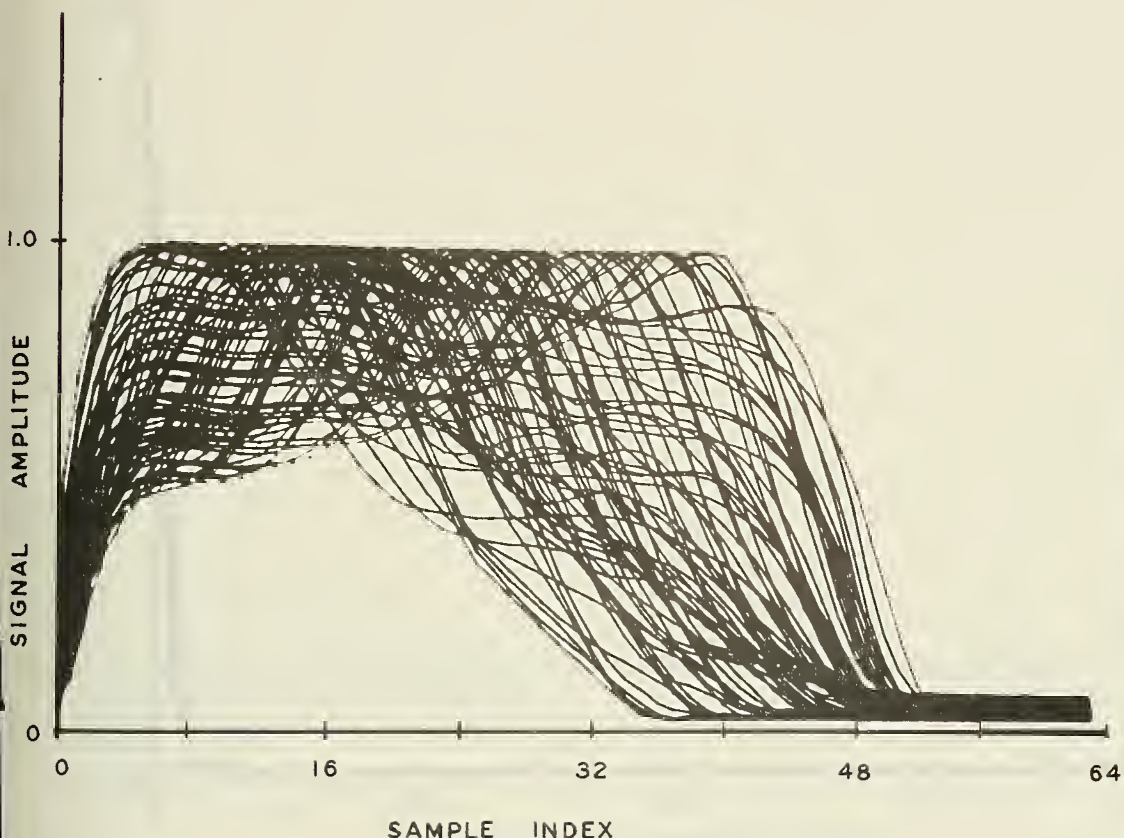

Figure 10. Overlaid Plots of the Prototype Signals of 79 Classes

Figure 11. Overlaid Plots of the Fourier Prototypes of 79 Classes

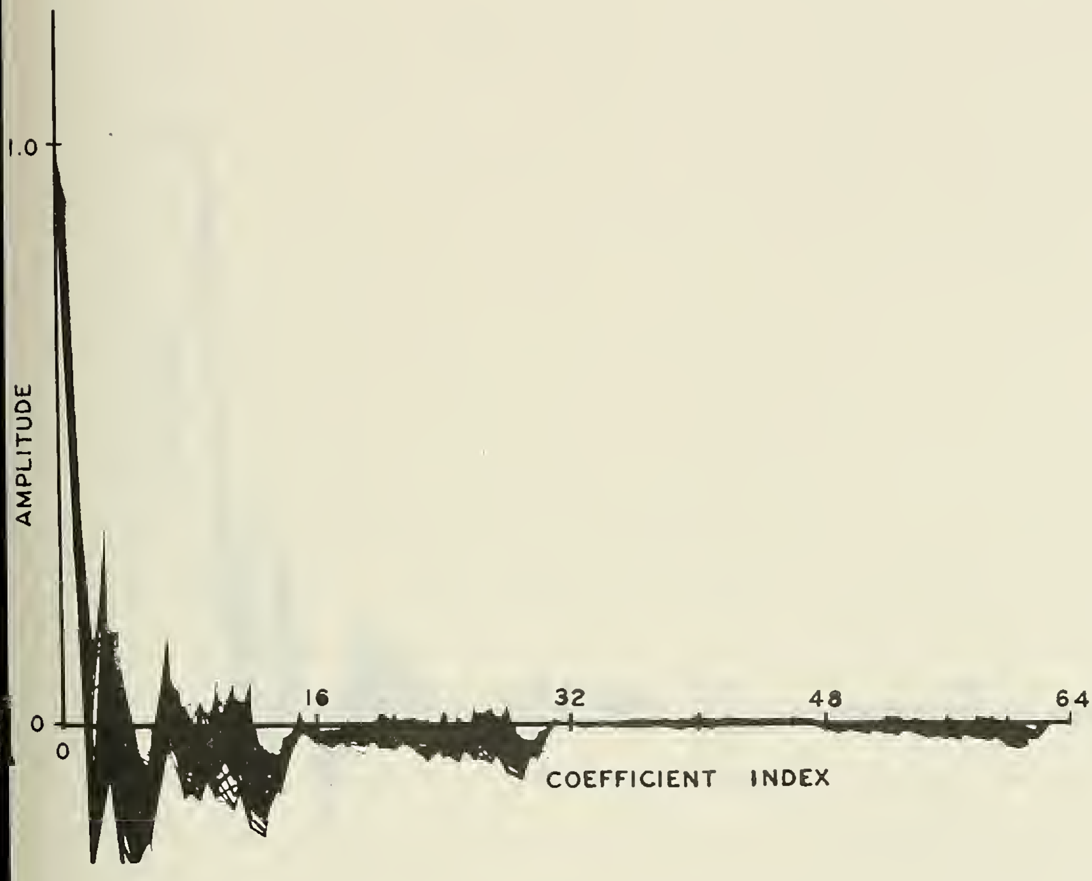

Figure 12. Overlaid Plots of the Walsh Prototypes of 79 Classes

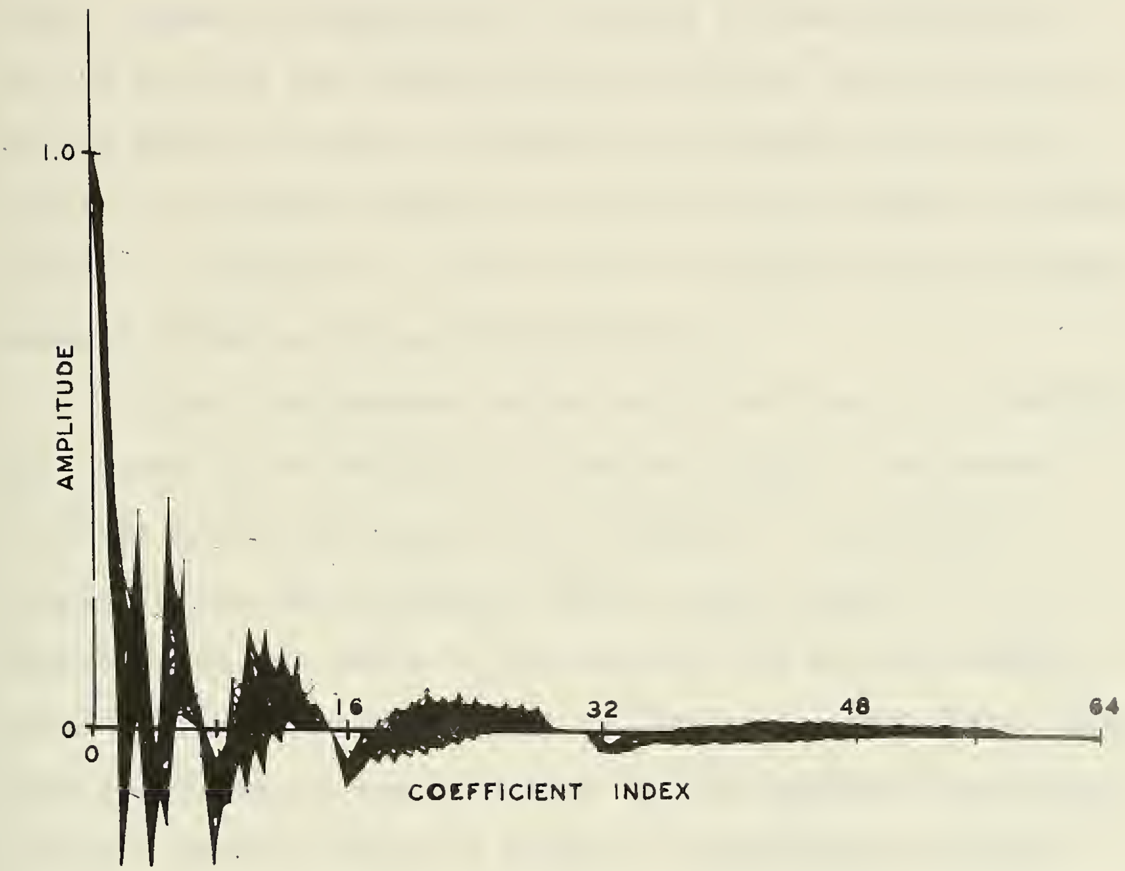

Figure 13. Overlaid Plots of the Haar Prototypes of 79 Classes

rank of magnitude in test results, not in original coefficient index order. Tables D1 to D10 of Appendix D list the numerical values in both original coefficient and rank order.

1. Comments on Signal Data

Before a meaningful comparison of any data can be made it must be normalized or scaled to some reference. In the case of the transform coefficients, this reference is the zero-th order coefficient or average value of the signal. The same reference is used in the feature selection tests. In Figure 10, each curve is scaled to have the same maximum value which may be misleading.

The superimposed curves show that there is considerable error in estimating the leading edge of the pulses from which the prototypes are estimated. By linearly extrapolating the estimated actual pulse origin, it is apparent that an error on the order of 8% of the average pulse width is present. That it appears in the class prototype indicates an inconsistency in the leading edge determination process which is manual. A threshold crossing decision would have minimized this error which undoubtedly affected the Walsh and Haar data due to the non-time-invariant nature of these transformations.

To illustrate the relative effects of time window jitter and quantizer noise, a pulse class (9-11) was selected at random for inspection of each signal and transform used to generate the class prototype. Figures 17 - 20 show the signal, Fourier, Walsh, and Haar coefficients of the class

as superimposed curves. In Figure 14 both time jitter and quantizing effects are apparent. The FFT data, Figure 18, shows no visible coefficient variation, while FWT and FHT data, Figures 19 and 20 respectively, show that some coefficients are quite noisy. The Haar functions of index 2^m, m=1, 2, ..., 5, are non-zero only during the first $64/2^m$ signal samples and thus reflect the effect of time jitter to the greatest extent in their respective coefficients.

Results of the F-Ratio test performed on the signal sample data for the 20 classes 6-11 through 10-12 (see Fig. 16) indicate that most of the information of classification value — as determined by this metric — is distributed fairly uniformly over 32 of the 64 samples. Figure 21 shows how the information for these classes is distributed in signal space (time) order. This is somewhat surprising in that the leading edge region is considered by this metric to be useless while the latter midsection and trailing edge region rates high. This result is believed due to the large variance in edge data caused by the time jitter mentioned above. The trailing edges are affected on an individual class basis rather than globally, which does not tend to lower the average for the whole ensemble. Given an accurate time-of-arrival (TOA) estimate it is conjectured that the leading edge region would rank high also. This would tend to increase the necessary dimensionality by including more samples in the "good feature" category.

2. Comments on Transform Data

Because of the magnitude operation on the Fourier sine and cosine pairs, the number of unique coefficients is reduced by half. This operation is time consuming but results in time-invariant features which, in light of the jitter present in the data base, would tend to favor the FFT in this comparison. Not so fortunate are the Walsh and Haar bases, both of which are affected by time reference variation. Figures 14 and 15 compare the information distributions in the three spaces while Figure 16 includes signal data as well.

From Figures 14 and 15 it is apparent that the Fourier basis has several clear advantages. Most of the useful information is in the first 12 coefficients. Not only is the information concentrated in a few features, but that information is a monotone decreasing function of index. Thus the order of the transform, N, and the time of execution can be reduced considerably. For an order reduction R, which is a power of 2. the number of arithmetic operations is reduced by $R \log_2 R$. For the case considered here the savings in arithmetic operations amounts to a reduction factor of 8.

The FWT and FHT data are difficult to interpret due to the time jitter. All Walsh coefficients are global in that they are functions of all signal data points, whereas all Haar coefficients except the first and second are local. See Appendix B. The first two Haar functions are identical to the first two sequency order Walsh functions and hence will generate identical coefficients.

Time jitter may have two effects on the FWT coefficients. It will certainly produce a variation in coefficient values which would reduce their effectiveness as classification features. Furthermore, in the case of higher order coefficients, this variation might tend to make the clustering multimodal. The variance ratio feature selection tests used in this work fail when clusters are not unimodal. This may explain why so many of the Walsh coefficients have large apparent information content.

The similarity of Haar functions to both Walsh functions and so-called block pulses (which are the set of basis functions for the signal space) is apparent in Figure 16. The Haar coefficient curve is similar to the Walsh coefficient curve for those features of high information content and to the signal sample curve for those of little apparent information.

Condensed correlation matrices for the three transform spaces are shown in Tables D11 to D13. Only the eight features having the highest classificatory information as determined by the 79 class F-Ratio test are included. Evident is a high degree of correlation between FWT and FHT coefficients which may be due to multimodal clustering or to poor resolution of a given signal detail by anything but an extended linear combination of Walsh or Haar basis functions. In this respect the Fourier basis also excels as evidenced by much smaller, but still considerable, inter-coefficient correlation. Once again, this may be due to the time invariance of the Fourier basis.

B. CONCLUSIONS

On the basis of the results of this investigation it is concluded that the Fourier basis as represented by the FFT can produce a dimensionality reduction factor of 5 or 6 for the signal data base employed. If actual pulse signal emitters of a common type display this degree of pulse shape dissimilarity then efficient classification should be possible on the basis of signal envelope shape. The effects of additive noise, multipath propagation, and signal distortion resulting from pulse-to-pulse amplitude variation and a nonlinear (square-law) detector were not investigated and would certainly degrade the value of the selected features for classification purpose.

No positive conclusions can be drawn from the Walsh and Haar transform results due to the jitter present in the signal data base. Further investigation may show that in the absence of time window jitter one of these transforms may exhibit the capability for dimensionality reduction to an extent that its use as a feature generator is feasible. The fact that the FWT and FHT are extremely fast makes them highly desirable for real-time processing.

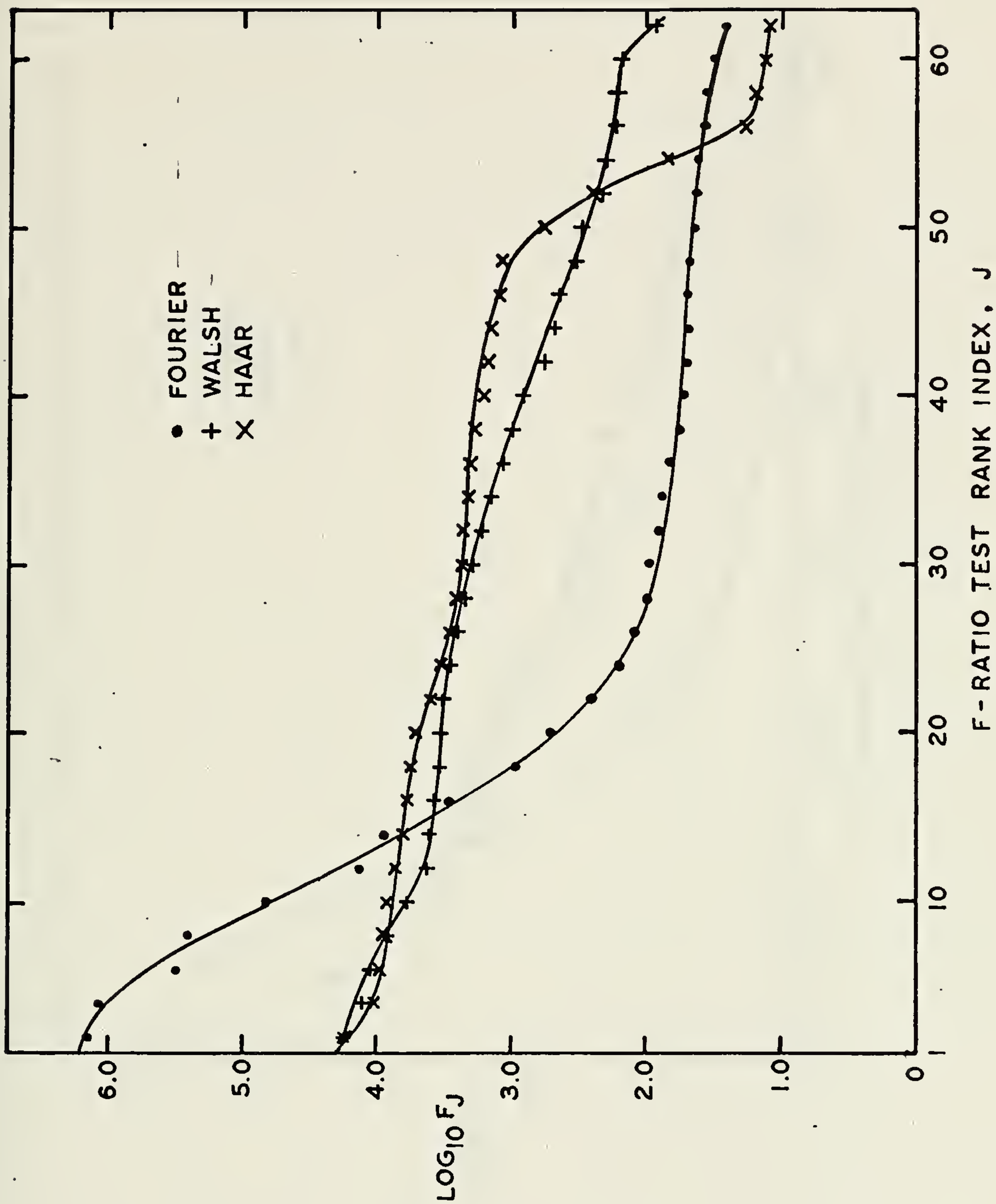

Figure 14. F-Ratio Test Information Measure of Representations in Three Bases for all 79 Classes as Functions of Test Rank Index

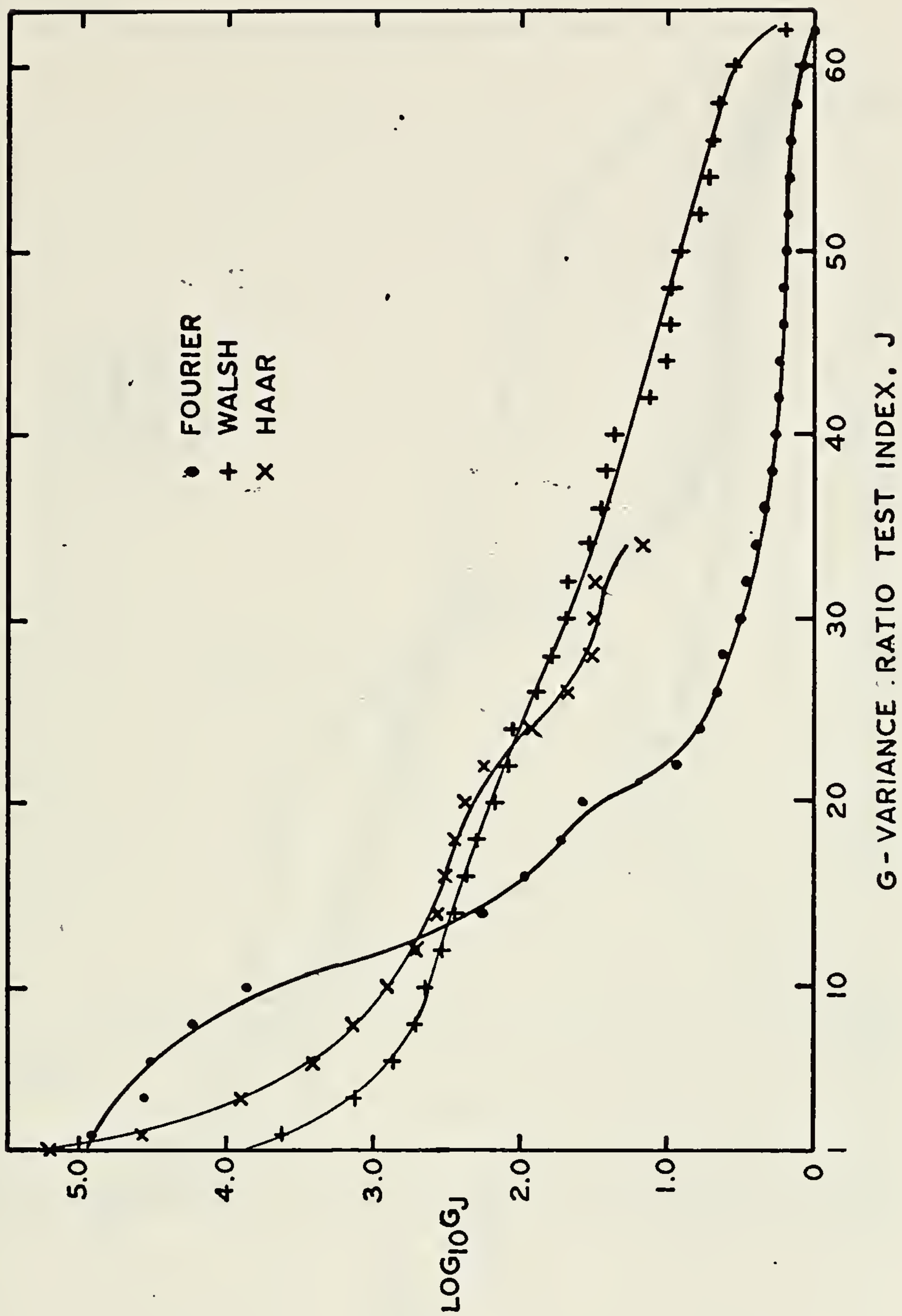

Figure 15. G-Variance Ratio Test Information Measure of Representations in Three Bases for all 79 Classes as Functions of Test Rank Index

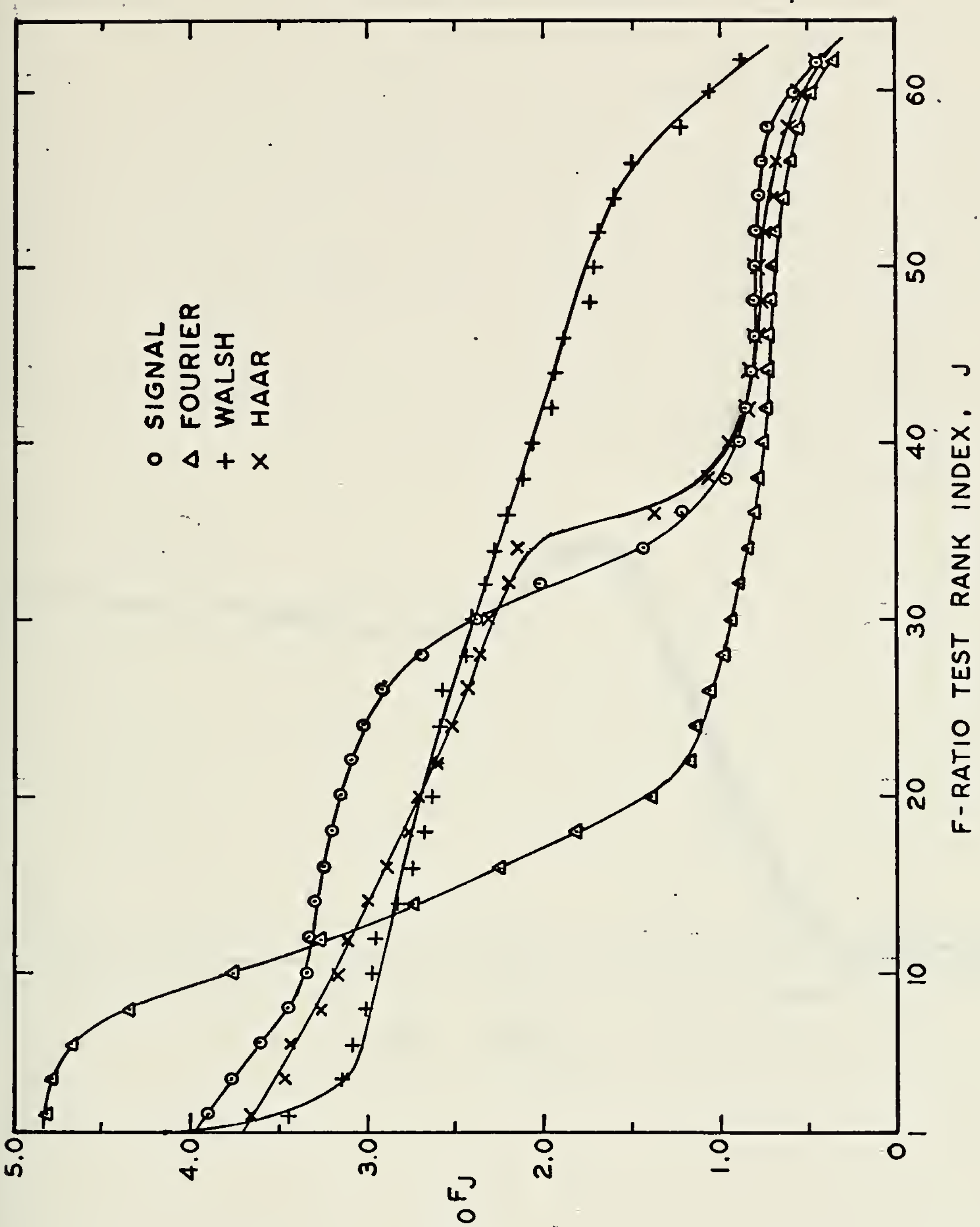

Figure 16. F-Ratio Test Information Measure of Four Basis Representations for 20 Classes (6-11 to 10-12) as Functions of Test Rank Index

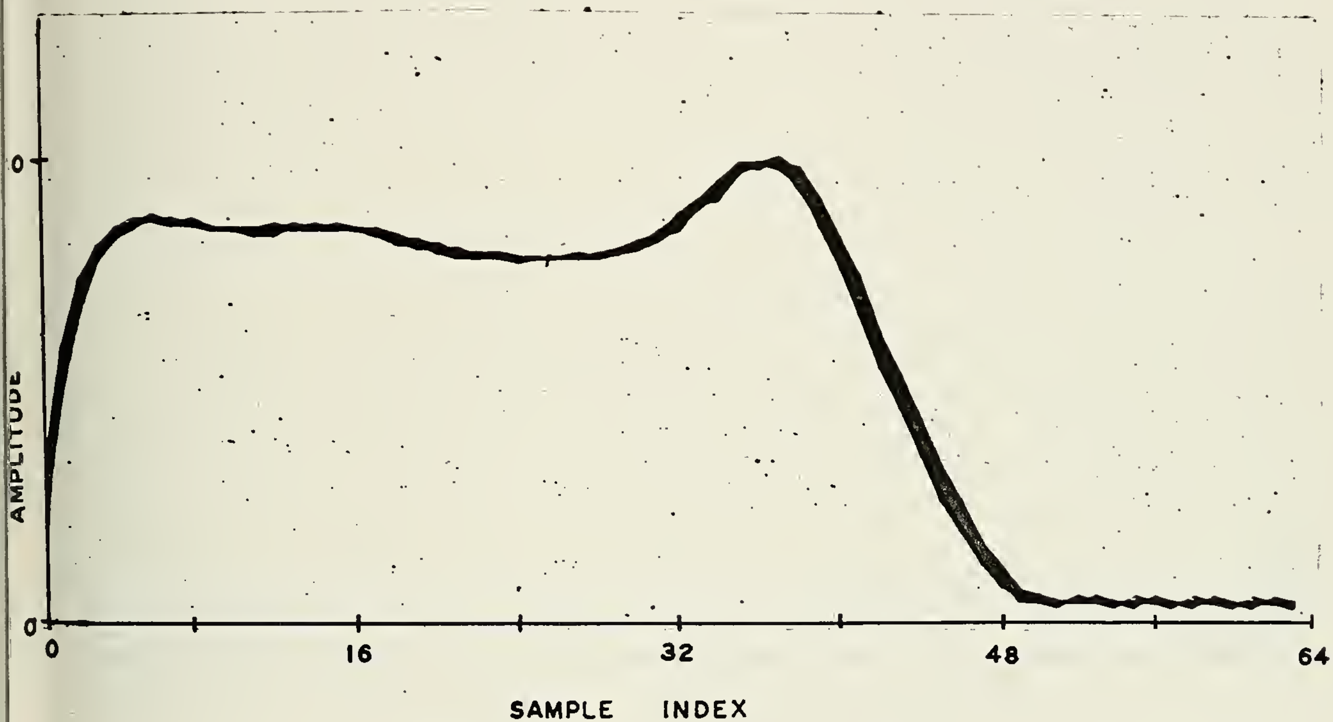

Figure 17. Overlaid Plots of the 25 Signals Defining Class 9-11

Figure 18. Overlay of the 25 Sets of FFT Coefficients of the Signals Defining Class 9-11

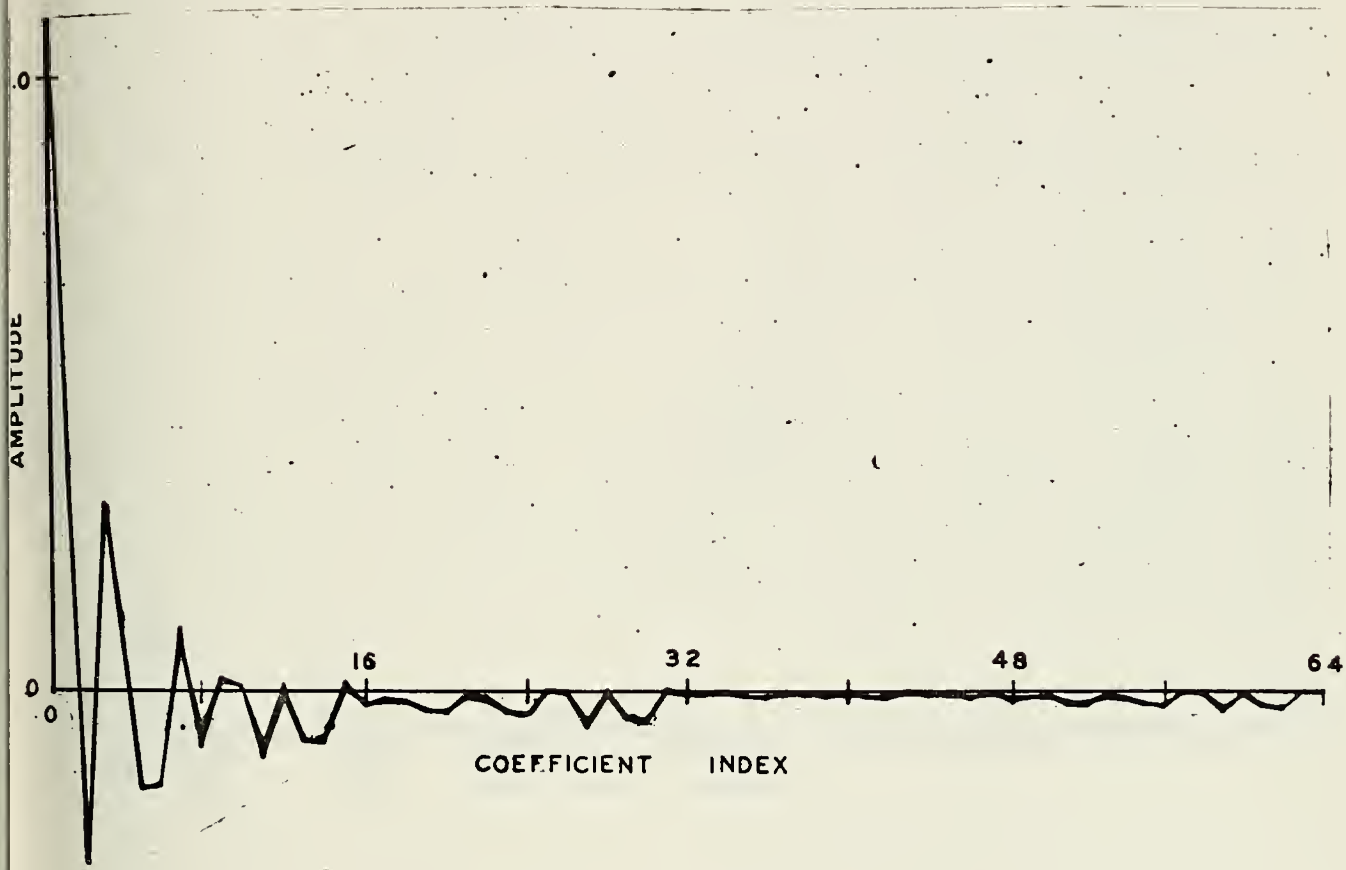

Figure 19. Overlay of the 25 Sets of FWT Coefficients of the Signals Defining Class 9-11

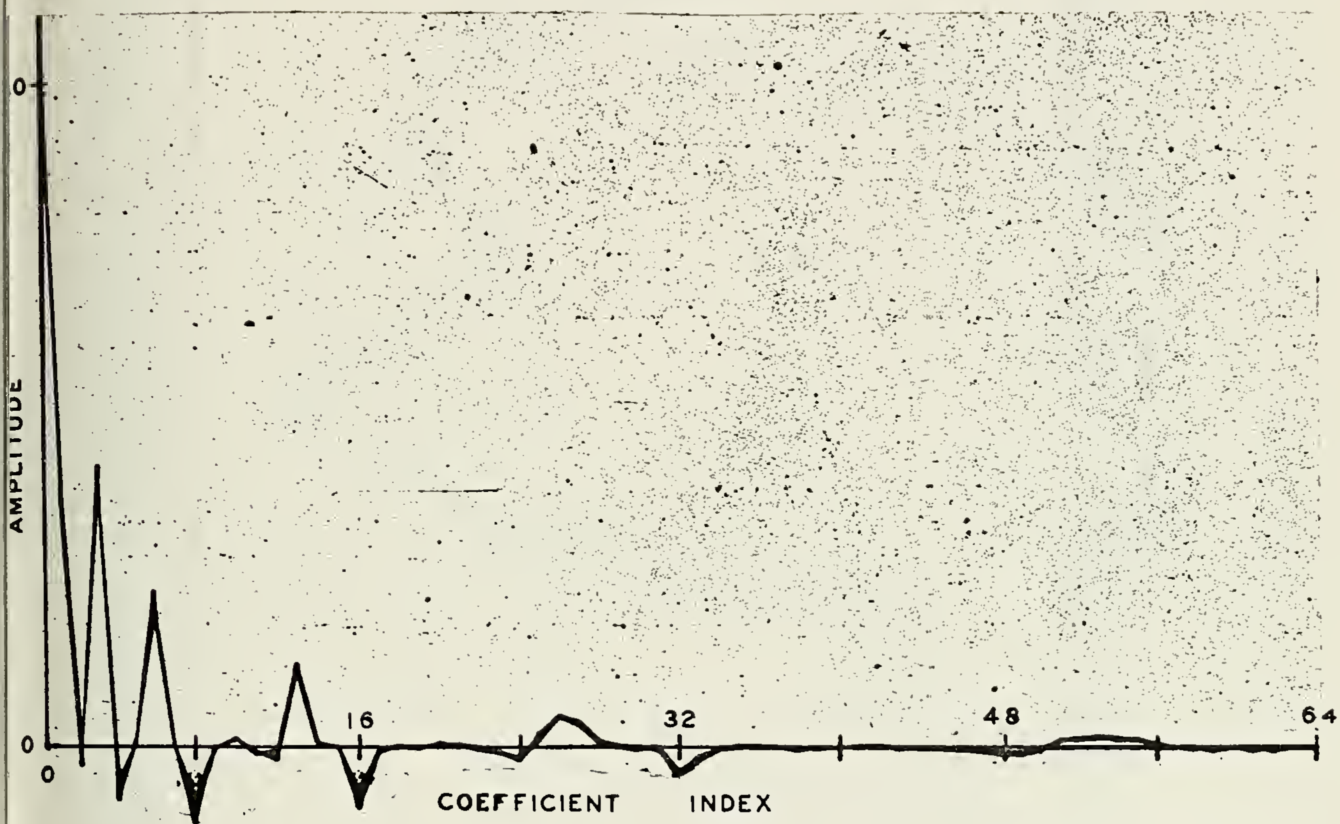

Figure 20. Overlay of the 25 Sets of FHT Coefficients of the Signals Defining Class 9-11

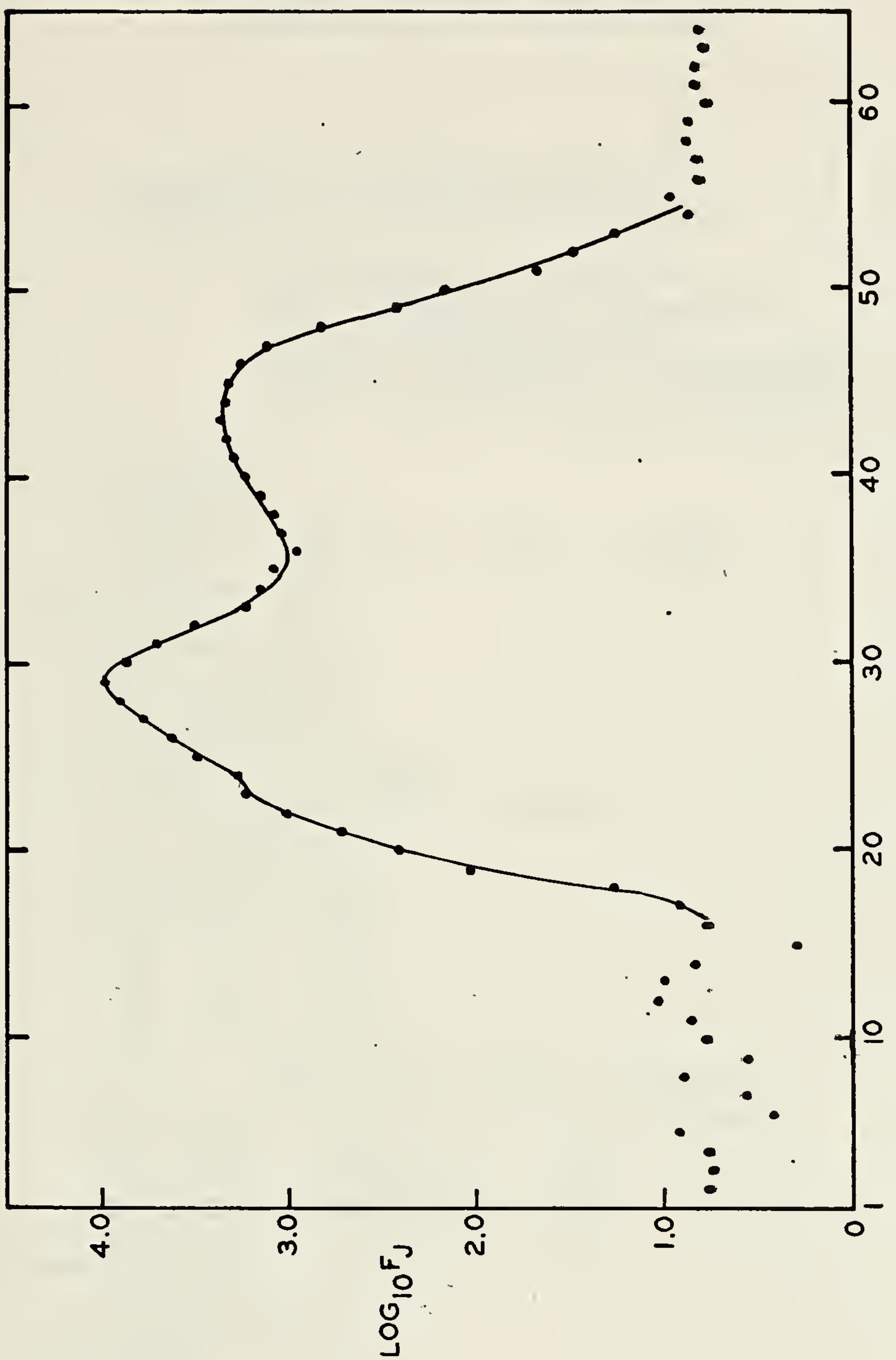

Figure 21. F-Ratio Test Information Measure of Signal Samples for 20 Classes (6-11 to 10-12) as a Function of Sample Index

APPENDIX A

LISTING OF FAST SUBROUTINES

```
FTN
      SUBROUTINE  FFT(M,REAL,SIGNF)
      DIMENSION S(2,64),RIM(64),REAL(64)
C
C              FAST FOURIER TRANSFORM
C              M - LOG2(NOMBER OF SAMPLES)
C              REAL - I/O ARRAY
C              SIGNF - DIRECTION OF TRANSFORM
C              OUT PUT IS IN MAGNITUDE SQUARED FORM
C
      N = 2**M
      NHALF = N / 2
      FLOTN = N
      PIARG = 6.2831853 / FLOTN * SIGNF
      DO 1000 I=1,N
 1000 RIM(I) = 0
      DO 3000 I=1,M
      N2I = 2**(M-I)
      NI = 2**(I-1)
      DO 2000 J=1,NI
      IN2I = (J-1) * N2I
      THETA = FLOAT(IN2I) * PIARG
      C = COS(THETA)
      SI = SIN(THETA)
      DO 2000 K=1,N2I
      IN0 = K + IN2I
      IN1 = K + 2*IN2I
      IN2 = IN1 + N2I
      IN3 = IN0 + NHALF
C              COMPLEX MULTIPLY
      CR = C * REAL(IN2)  -  SI * RIM(IN2)
      CI = SI * REAL(IN2)  +  C * RIM(IN2)
      S(1,IN0) = REAL(IN1)  +  CR
      S(2,IN0) = RIM(IN1)  +  CI
      S(1,IN3) = REAL(IN1)  -  CR
      S(2,IN3) = RIM(IN1)  -  CI
 2000 CONTINUE
      DO 3000 L=1,N
      REAL(L) = S(1,L)
      RIM(L) = S(2,L)
 3000 CONTINUE
C              COMPUTE MAGNITUDE SQUARED
      DO 4000 I=1,N
 4000 REAL(I) = REAL(I)*REAL(I)  +  RIM(I)*RIM(I)
      RETURN
      END
```

```
      FTN
            SUBROUTINE FWT(M,X)
            DIMENSION X(1)
      C                 FAST WALSH XFORM
      C                 M - LOG2(N)
      C                 N - NUMBER OF SAMPLES
      C                 X - I/O ARRAY: (1:N)=I/O; (N+1:2N)=SCRATCH
            N = 2**M
            NH = N / 2
            LR = 0
            DO 1000 L=1,M
            LP = L + 1
            LM = L - 1
            LR = N - LR
            LT = N - LR
            NY = 0
            NZ = 2**LM
            NZI = 2 * NZ
            NZN = N / NZI
            DO 1000 I=1,NZN
            NX = NY + 1
            NY = NY + NZ
            JS = (I-1) * NZI
            JD = JS + NZI + 1
            DO 1000 J=NX,NY
            JS = JS + 1
            JT = J + NH
            LJS = LR + JS
            LTJ = LT + J
            LTJT = LT + JT
            X(LJS) = X(LTJ) + X(LTJT)
            JD = JD - 1
            LJD = LR + JD
       1000 X(LJD) = X(LTJ) - X(LTJT)
            IF ( LR ) 1500,3000,1500
       1500 DO 2000 I=1,N
            IPN = I + N
       2000 X(I) = X(IPN)
       3000 RETURN
            END
```

```
FTN
      SUBROUTINE FHT(M,S)
      DIMENSION S(64),H(64)
C
C             FAST HAAR TRANSFORM
C
C                  M - LOG2(NR OF DATA POINTS)
C                  S - I/O VECTOR OF LENGTH 2**M
C                  H - SCRATCH VECTOR
C
C             FHT REQUIRES 2(N-1) REAL ADD OPERATIONS
C
      N=2**M
      NH=N
      DO 4000 I=1,M
      NH=NH/2
      DO 1000 J=1,NH
      I1=J
      I2=J+NH
      J2=2*J
      J1=J2-1
      H(I1)=S(J1)+S(J2)
      H(I2)=S(J1)-S(J2)
 1000 CONTINUE
      NH2=NH*2
      DO 2000 J=1,NH2
      S(J)=H(J)
 2000 CONTINUE
      GO TO (4000,3000)I
 3000 NH21=NH2+1
      DO 4000 J=NH21,N
      S(J)=S(J)*1.414213562
 4000 CONTINUE
      RETURN
      END
```

APPENDIX B

WALSH AND HAAR FUNCTIONS AND MATRICES

The increasingly familiar Walsh functions and the less well known Haar functions originated in the early 20th century. J. A. Barrett, as described by Fowle [11] was perhaps the first to discover Walsh functions, using them as the basis of a telegraph wire transposition scheme to reduce crosstalk. J. L. Walsh in 1923 [12] formalized the set of complete orthogonal bivalued functions defined on the unit interval [0,1] which now bear his name. An important orthogonal but incomplete subset of the Walsh functions are the square-waves known as Rademacher functions after H. A. Rademacher [13], who developed them as part of a unified theory of orthogonal functions in the early 20's.

Much of the recent interest in application of Walsh functions was stimulated by their adaptability to digital processing. For example, a discrete Walsh matrix, like the discrete Fourier matrix of sampled sinusoids, contains the symmetry and redundancy required for a fast transform algorithm based on matrix factorization. Because of the bivalued nature of the functions, the fast Walsh transform or any Walsh function based processing is inherently suited to digital implementation. Harmuth [14] proposes many and varied uses for Walsh functions in applications from signal processing to communication data multiplexing.

The set of Walsh functions of order $N = 2^n$ for all non-negative integers, n, forms an Abelian group under multiplication. That is, the product, equi-argument wise, of any two functions of the set is another member of the set. The first eight Walsh functions are shown below in Figure 22.

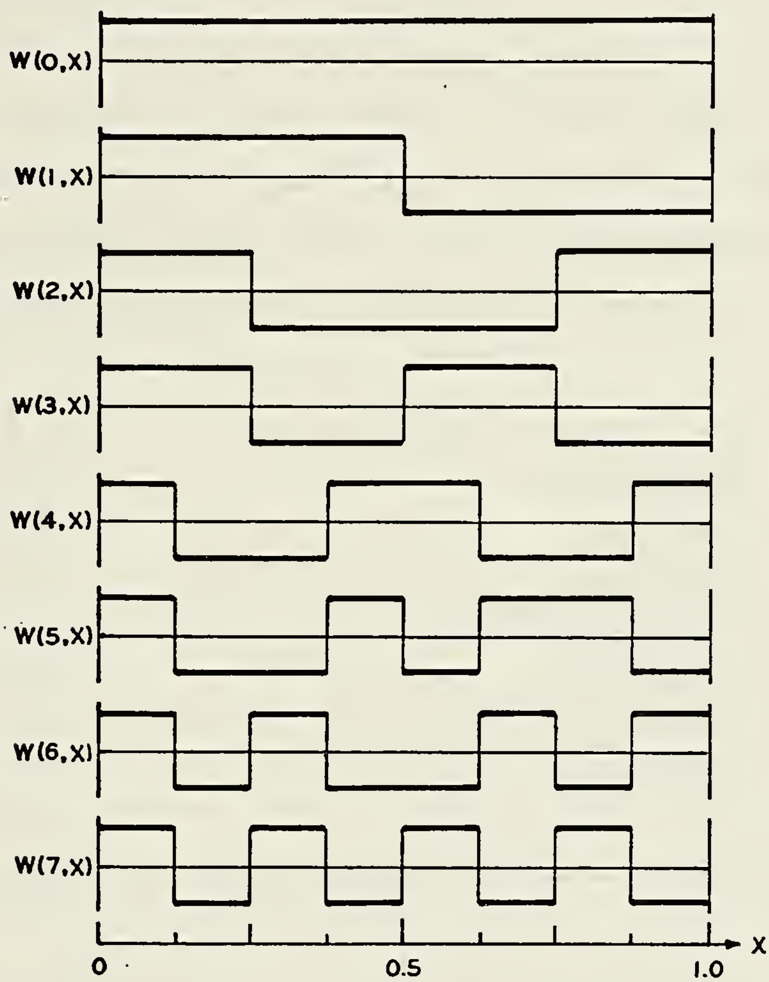

Figure 22. Continuous Walsh Functions of Order 8

The ordering shown here is the so-called sequency order after Harmuth who defines sequency as the average number of zero crossings per unit interval, (0,1).

Harmuth chooses to define the Walsh functions on $[-\frac{1}{2},+\frac{1}{2}]$ and employs the notation Cal(s,x), Sal(s,x) to accentuate the symmetry similarities to the sinusoidal trigonometric functions. Sequency, s, is now defined as one-half the average number of zero crossings per unit interval $[-\frac{1}{2},+\frac{1}{2})$.

The discrete Walsh functions, $W_n(i,k)$, i = 0,1,...,N-1 and k = 0,1,...,N-1 are formed by sampling the continuous Walsh functions at N equally spaced points on the interval of definition. The discrete form is most conveniently shown in matrix form as in Figure 23, below.

$$\underset{\sim}{W}_8 = \begin{bmatrix} + & + & + & + & + & + & + & + \\ + & + & + & + & - & - & - & - \\ + & + & - & - & - & - & + & + \\ + & + & - & - & + & + & - & - \\ + & - & - & + & + & - & - & + \\ + & - & - & + & - & + & + & - \\ + & - & + & - & - & + & - & + \\ + & - & + & - & + & - & + & - \end{bmatrix} = \begin{bmatrix} W_8(0,k) \\ W_8(1,k) \\ W_8(2,k) \\ W_8(3,k) \\ W_8(4,k) \\ W_8(5,k) \\ W_8(6,k) \\ W_8(7,k) \end{bmatrix}$$

Figure 23. Walsh Sequency Matrix of Order 8

The Haar functions form a complete orthogonal but non-orthonormal set of bivalued functions on [0,1], and were first published by A. Haar in 1909 [15]. This set is related to the set of Walsh functions as pointed out by Fino [6],

but appear considerably different. The orthogonal Haar functions attain values +1, -1, and 0 as shown below in Figure 24, which clearly illustrates the increasingly local nature of higher orders. The literature indexes Haar functions by a subscript and a superscript, a system which provides insight to the shape of a function from its indices but is somewhat clumsy for this work which employs a single subscript index.

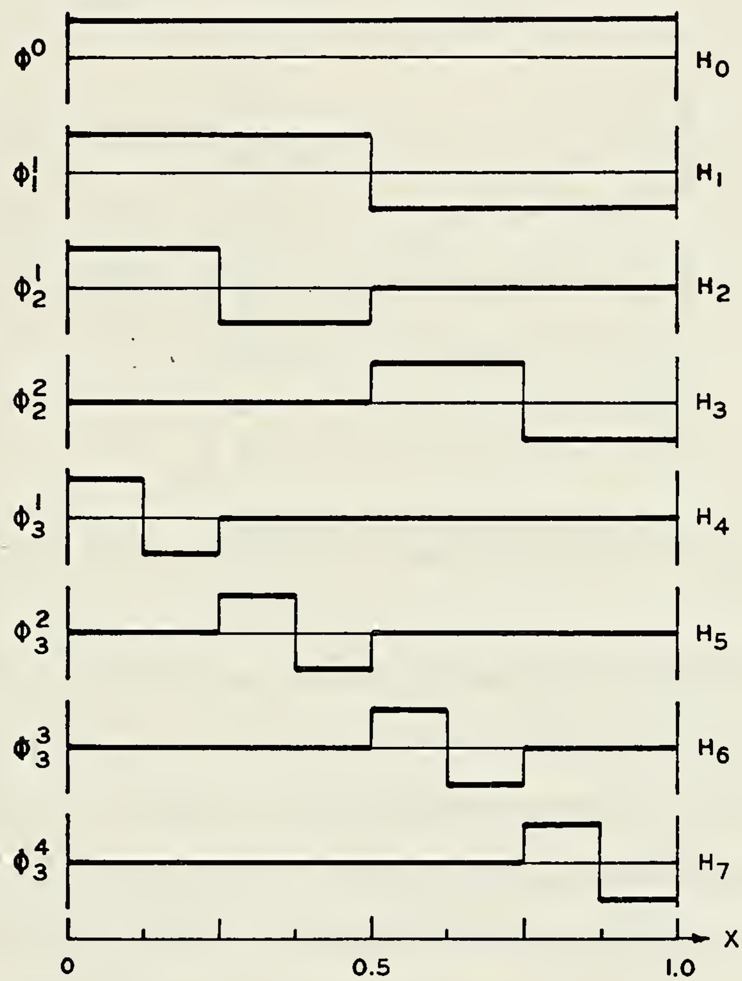

Figure 24. Continuous Haar Functions of Order 8

This orthogonal set may be normalized by multiplying each orthogonal function by $(\sqrt{2})^{k-1}$ where k is the sub-index in ϕ_k^j.

The discrete Haar functions of order N are formed, like the discrete Walsh functions, by sampling the continuous functions at N equally spaced points on the interval of definition. The N-square Haar matrix formed of the first N discrete Haar functions is shown in Figure 25 in orthogonal form.

$$\underset{\sim}{H}_8 = \begin{bmatrix} + & + & + & + & + & + & + & + \\ + & + & + & + & - & - & - & - \\ + & + & - & - & 0 & 0 & 0 & 0 \\ 0 & 0 & 0 & 0 & + & + & - & - \\ + & - & 0 & 0 & 0 & 0 & 0 & 0 \\ 0 & 0 & + & - & 0 & 0 & 0 & 0 \\ 0 & 0 & 0 & 0 & + & - & 0 & 0 \\ 0 & 0 & 0 & 0 & 0 & 0 & + & - \end{bmatrix}$$

Figure 25. Orthogonal Haar Matrix of Order 8

Both Walsh and Haar matrices contain high redundancy which has led to not only the fast transform algorithms but to a variety of generating methods based on their internal symmetry, [6], [16]-[20]. The fast Walsh and Haar algorithms used in this research are adapted from papers by Robinson [18] and Rejchrt [20] respectively.

APPENDIX C

GENERALIZED FOURIER SERIES

Consider the infinite dimensional signal (vector) space, S, consisting of all continuous physically realizable signals (functions) defined on $a \leq x \leq b$. On this space is defined an inner product or projection operation

$$\underset{\sim}{f} \bullet \underset{\sim}{g} = \int_a^b f(x)g(x)\,dx.$$

S contains orthonormal systems of infinitely many vectors. Let $E = \{\underset{\sim}{e}_0, \underset{\sim}{e}_1, \ldots, \underset{\sim}{e}_n, \ldots\}$ be one such system. The orthonormality condition states that the $\underset{\sim}{e}_i$ satisfy

$$\underset{\sim}{e}_i \bullet \underset{\sim}{e}_j = \delta_{ij} = \begin{matrix} 0 \text{ for } i \neq j \\ 1 \text{ for } i = j \end{matrix}$$

for all non-negative integer indices i and j.

An arbitrarily chosen signal, s(x), in S can be represented by sequentially nested subsets of E, each of which spans a subspace of S. For clarity it should be noted that any segment of the real line can be considered an infinite dimensional vector space, hence s(x) can be expressed as $\underset{\sim}{s}$, depending on the context.

The signal (vector) $\underset{\sim}{s}$ possesses a "best" S_1 approximator $\underset{\sim}{s}_1$ in the subspace S_1 spanned by E_1 and is given by $\underset{\sim}{s}_1 = p_0\underset{\sim}{e}_0$, where $p_0 = (\underset{\sim}{s} \bullet \underset{\sim}{e}_0)$ is the projection of $\underset{\sim}{s}$ onto $\underset{\sim}{e}_0$. In other

words, $p_0 \underset{\sim}{e}_0$ is the vector in E_1 which is by some measure closest to $\underset{\sim}{s}$ of all vectors in E_1. Similarly, $\underset{\sim}{s}$ possesses a "best" S_2 approximator in E_2

$$\underset{\sim}{s}_2 = p_0 \underset{\sim}{e}_0 + p_1 \underset{\sim}{e}_1$$

$$= (\underset{\sim}{s} \cdot \underset{\sim}{e}_0) \underset{\sim}{e}_0 + (\underset{\sim}{s} \cdot \underset{\sim}{e}_1) \underset{\sim}{e}_1$$

and a "best" S_k approximator computed in the same manner in $E_k = \{\underset{\sim}{e}_0, \underset{\sim}{e}_1, \underset{\sim}{e}_2, \ldots, \underset{\sim}{e}_{k-1}\}$, that is,

$$\underset{\sim}{s}_k = p_0 \underset{\sim}{e}_0 + p_1 \underset{\sim}{e}_1 + \ldots + p_{k-1} \underset{\sim}{e}_{k-1}.$$

By virtue of the orthogonality of the $\underset{\sim}{e}_i$, each coefficient p_i is invariant in the S_k approximations for $k \geq i = 0, 2, \ldots$. The limiting approximator,

$$\lim_{n\to\infty} S_n = \lim_{n\to\infty} \sum_{j=0}^{N} (\underset{\sim}{s} \cdot \underset{\sim}{e}_j) \underset{\sim}{e}_j$$

is called the Fourier E-coefficient expansion of $\underset{\sim}{s}$, and the coefficients $p_j = (\underset{\sim}{s} \cdot \underset{\sim}{e}_j)$ are the Fourier E-coefficients.

As implied above, a Fourier E-coefficient expansion of $\underset{\sim}{s}$ has the property that for each successive $k = 1, 2, \ldots$, the S_k approximator formed of the first k terms is "best" in the sense that there is no other vector "closer" to $\underset{\sim}{s}$ in the subspace S_k. Implicit here is that $\underset{\sim}{s}_k$ is <u>at least</u> as good as $\underset{\sim}{s}_{k-1}$.

"Closest" as used here is in the sense of Euclidean distance or the norm of the difference between the two vectors $\underset{\sim}{s}$ and $\underset{\sim}{s}_k$. "Best" implies that $\underset{\sim}{s}_k$ is the closest of all S_k approximators to $\underset{\sim}{s}$. To formalize the notion, the distance is given by

$$\|\underset{\sim}{s} - \underset{\sim}{s}_k\| = (\underset{\sim}{s} - \underset{\sim}{s}_k) \bullet (\underset{\sim}{s} - \underset{\sim}{s}_k) .$$

To prove that $\underset{\sim}{s}_k$ is the best S_k approximator of $\underset{\sim}{s}$ in the norm, choose an arbitrary S_k approximator

$$\underset{\sim}{s}'_k = \sum_{j=0}^{k-1} p'_j \underset{\sim}{e}_j ,$$

and determine the coefficients p'_j which makes the norm $\|\underset{\sim}{s} - \underset{\sim}{s}'_k\|$ smallest, or equivalently, minimizes $\|\underset{\sim}{s} - \underset{\sim}{s}'_k\|^2$.

$$\begin{aligned}\|\underset{\sim}{s} - \underset{\sim}{s}'_k\|^2 &= (\underset{\sim}{s} - \underset{\sim}{s}'_k) \bullet (\underset{\sim}{s} - \underset{\sim}{s}'_k) \\ &= \underset{\sim}{s} \bullet \underset{\sim}{s} - 2 \sum_{j=0}^{k-1} p'_j (\underset{\sim}{s} \bullet \underset{\sim}{e}_j) + \sum_{i=0}^{k-1} \sum_{j=0}^{k-1} p'_i p'_j (\underset{\sim}{e}_i \bullet \underset{\sim}{e}_j) \\ &= \|\underset{\sim}{s}\|^2 - 2 \sum_{j=0}^{k-1} p'_j p_j + \sum_{j=0}^{k-1} (p'_j)^2 \\ &= \|s\|^2 + \sum_{j=0}^{k-1} (p'_j - p_j) - \sum_{j=0}^{k-1} (p_j)^2 .\end{aligned}$$

Thus $p'_j = p_j = \underset{\sim}{s} \bullet \underset{\sim}{e}_j$, $j = 0, 1, 2, \ldots, k-1$ is the coefficient set which results in the best S_k approximator.

The limiting case of the best S_k approximator does not imply that $\lim_{k\to\infty} \|\underset{\sim}{s} - \underset{\sim}{s}_k\| = 0$. It is conceivable that we can find an $\underset{\sim}{s}$ which possesses components which are orthogonal to every vector in the infinite set E. One example is the infinite system

$$E = \left\{ \frac{1}{2\pi} , \frac{1}{2\pi} \sin(x) , \frac{1}{2\pi} \sin(2x) , \ldots \right\}$$

spanning the space of continuous functions defined on $-\pi \leq x \leq \pi$. E is orthonormal and infinite, yet the best S_k approximator for $f(x) = A\cos(x)$ is zero for all k. This introduces the notion of completeness. An infinite orthonormal system E is said to be a complete orthonormal system if for every $\underset{\sim}{s} \in S$, the norm $\|\underset{\sim}{s} - \underset{\sim}{s}_k\| \to 0$ as $k \to \infty$.

To this point the discussion has been limited to continuous signal and infinite dimensional signal (vector) spaces. The results can be modified to cover finite dimensional, say N, signal spaces which are not unbounded, that is, the set of N-dimensional vectors whose elements are real numbers possible obtained by sampling the value of continuous functions at N equally spaced points on the interval $a \leq x \leq b$. It is implicitly assumed that the constraints placed by the sampling theorem are met.

We define a discrete inner product operation on the space S_N as

$$\underset{\sim}{F}_N \bullet \underset{\sim}{G}_N = \sum_{n=0}^{N-1} f_n g_n = \underset{\sim}{F}_N \underset{\sim}{G}_N^T$$

where $\underset{\sim}{F}_N = (f_0, f_1, \ldots, f_{N-1})$ and $\underset{\sim}{G}_N = (g_0, g_1, \ldots, g_{N-1})$. Let $D_N = \{\underset{\sim}{d}_0, \underset{\sim}{d}_1, \ldots, \underset{\sim}{d}_{N-1}\}$ be a discrete N-dimensional orthonormal system spanning S_N. The $\underset{\sim}{d}_n$ are 1xN vectors satisfying

$$\underset{\sim}{d}_i \bullet \underset{\sim}{d}_j = \underset{\sim}{d}_i \underset{\sim}{d}_j^T = \delta_{ij} \quad .$$

For any signal vector in S_N, say $\underset{\sim}{s} = (s_0, s_1, \ldots, s_{N-1})$ there is a best S_k approximator in the norm given by

$$\underset{\sim}{s}_k = \sum_{i=0}^{k-1} p_i \underset{\sim}{d}_i \quad \text{for all } k = 1, 2, \ldots, N$$

where

$$p_i = \underset{\sim}{s} \bullet \underset{\sim}{d}_i = \underset{\sim}{s}\, \underset{\sim}{d}_i^T = \sum_{j=1}^{N-1} \underset{\sim}{s}_j\, \underset{\sim}{d}_{ji} \quad .$$

The N-dimensional system D_N is said to be a complete discrete orthonormal system if for every $\underset{\sim}{s} \epsilon S_N$, the norm $\| \underset{\sim}{s} - \underset{\sim}{s}_k \| = 0$.

In the above discussion, general orthonormal systems spanning continuous and discrete signal spaces have been considered. Nothing has been said about which orthonormal system or basis may be best suited to representation of a certain category of signals in the space.

A given signal, $\underset{\sim}{v}$, in the discrete signal space S_N possesses best S_k approximators in every orthonormal basis in S_N. However the best S_k approximator in one basis will in general posses a greater or smaller norm error than the best S_k approximator in another basis. Since there is an

infinite number of signals possible in S_N, the determination of the best orthonormal basis to represent a particular category of signals by a truncated series, that is a S_k approximator, is more than a casual matter.

APPENDIX D

TABULATION OF NUMERICAL RESULTS

SIGNAL SPACE 6-11 TO 1Ø-12

F-RATIO VECTOR. NR SIG PER CLASS = 25 NR CLASSES = 2Ø

N	GLOBAL MEAN	F - RATIO	RANK	F - RATIO
1	.222Ø7Ø3Ø7	.55Ø55E+Ø1	28	.93782E+Ø4
2	.286132872	.57295E+Ø1	27	.73377E+Ø4
3	.323Ø46923	.57926E+Ø1	29	.69ØØ4E+Ø4
4	.341Ø74228	.8Ø339E+Ø1	26	.58Ø17E+Ø4
5	.347714841	.27556E+Ø1	3Ø	.5ØØ5ØE+Ø4
6	.351523519	.369Ø8E+Ø1	25	.4Ø367E+Ø4
7	.349199176	.7566ØE+Ø1	24	.31Ø68E+Ø4
8	.347734392	.5334ØE+Ø1	31	.3Ø961E+Ø4
9	.343847632	.59935E+Ø1	41	.22867E+Ø4
1Ø	.342832Ø29	.67135E+Ø1	43	.22955E+Ø4
11	.341581941	.1Ø259E+Ø2	42	.21555E+Ø4
12	.3426758Ø5	.9777ØE+Ø1	23	.21429E+Ø4
13	.344257712	.65Ø22E+Ø1	39	.18825E+Ø4
14	.34414Ø649	.19725E+Ø1	4Ø	.18669E+Ø4
15	.344668Ø31	.58Ø23E+Ø1	44	.17171E+Ø4
16	.344ØØ3975	.79927E+Ø1	22	.16895E+Ø4
17	.341718793	.2964ØE+Ø2	32	.16522E+Ø4
18	.337812543	.14Ø92E+Ø3	38	.16Ø63E+Ø4
19	.336386681	.25212E+Ø3	33	.13857E+Ø4
2Ø	.334472597	.66148E+Ø3	45	.13855E+Ø4
21	.3346Ø9389	.1Ø338E+Ø4	34	.12911E+Ø4
22	.338437557	.16895E+Ø4	37	.12444E+Ø4
23	.346464813	.21429E+Ø4	36	.11757E+Ø4
24	.356Ø15623	.31Ø68E+Ø4	21	.1Ø338E+Ø4
25	.3674Ø2315	.4Ø367E+Ø4	35	.95942E+Ø3
26	.38ØØ39Ø96	.58Ø17E+Ø4	46	.89299E+Ø3
27	.391523421	.73377E+Ø4	2Ø	.66148E+Ø3
28	.4Ø1757836	.93782E+Ø4	47	.5Ø426E+Ø3
29	.4Ø8632874	.69ØØ4E+Ø4	19	.25212E+Ø3
3Ø	.411835968	.5ØØ5ØE+Ø4	48	.25Ø78E+Ø3
31	.41Ø82Ø3Ø5	.3Ø961E+Ø4	18	.14Ø92E+Ø3

TABLE D1. Feature Selector (F-Ratio) Test on Signal Samples of 20 Classes (6-11 to 10-12)

SIGNAL SPACE (CONT)

32	.405371070	.16522E+04	49	.10401E+03
33	.395800829	.13857E+04	50	.44918E+02
34	.381640673	.12911E+04	17	.29640E+02
35	.365371048	.95942E+03	51	.17336E+02
36	.346074224	.11757E+04	52	.16858E+02
37	.322753906	.12444E+04	11	.10259E+02
38	.298769534	.16063E+04	12	.97770E+01
39	.270624995	.18825E+04	54	.84328E+01
40	.242421865	.18669E+04	4	.80339E+01
41	.213886738	.22867E+04	16	.79927E+01
42	.185917914	.21555E+04	7	.75660E+01
43	.158691436	.22955E+04	57	.69157E+01
44	.133320332	.17171E+04	53	.68629E+01
45	.108823142	.13855E+04	58	.68517E+01
46	.086152345	.89299E+03	10	.67135E+01
47	.066230476	.50426E+03	13	.65022E+01
48	.048710942	.25078E+03	56	.63940E+01
49	.036562510	.10401E+03	61	.63207E+01
50	.029863276	.44918E+02	60	.62801E+01
51	.027402349	.17336E+02	55	.61496E+01
52	.026562501	.16858E+02	63	.61142E+01
53	.027324218	.68629E+01	62	.60556E+01
54	.027246099	.84328E+01	9	.59935E+01
55	.027187504	.61496E+01	15	.58023E+01
56	.027421873	.63940E+01	3	.57926E+01
57	.027285166	.69157E+01	2	.57295E+01
58	.027148437	.68517E+01	59	.56056E+01
59	.027460940	.56056E+01	1	.55055E+01
60	.027226567	.62801E+01	6	.36908E+01
61	.027226560	.63207E+01	8	.35340E+01
62	.027382810	.60556E+01	5	.27556E+01
63	.027246099	.61142E+01	14	.19725E+01

TABLE D1. (continued)

FOURIER 6-11 TO 10-12

F-RATIO VECTOR. NR SIG PER CLASS = 25 NR CLASSES = 20

N	GLOBAL MEAN	F - RATIO	RANK	F - RATIO
1	.150054395	.63360E+05	3	.64962E+05
2	.028901398	.49742E+05	1	.63360E+05
3	.007832460	.64962E+05	2	.49742E+05
4	.003212961	.21429E+05	4	.21429E+05
5	.002258407	.58363E+04	5	.58363E+04
6	.000839599	.14010E+04	6	.14010E+04
7	.000358398	.56836E+03	7	.56836E+03
8	.000244518	.17927E+03	8	.17927E+03
9	.000195182	.65161E+02	9	.65161E+02
10	.000114297	.23846E+02	10	.23846E+02
11	.000077852	.13883E+02	12	.14263E+02
12	.000054494	.14263E+02	11	.13883E+02
13	.000039765	.57374E+01	14	.11504E+02
14	.000030612	.11504E+02	30	.96354E+01
15	.000020852	.42061E+01	18	.84680E+01
16	.000016115	.38095E+01	26	.79446E+01
17	.000015180	.52134E+01	21	.73034E+01
18	.000011138	.84680E+01	20	.62571E+01
19	.000008543	.52743E+01	13	.57374E+01
20	.000009830	.62571E+01	23	.55700E+01
21	.000009220	.73034E+01	24	.53858E+01
22	.000008530	.49047E+01	28	.53833E+01
23	.000006571	.55700E+01	19	.52743E+01
24	.000006548	.53858E+01	17	.52134E+01
25	.000005893	.36414E+01	22	.49047E+01
26	.000005540	.79446E+01	27	.47574E+01
27	.000005772	.47574E+01	15	.42061E+01
28	.000004928	.53833E+01	16	.38095E+01
29	.000005287	.32960E+01	25	.36414E+01
30	.000006183	.96354E+01	29	.32960E+01
31	.000004341	.25476E+01	31	.25476E+01

TABLE D2. Feature Selector (F-Ratio) Test on Fourier Magnitude Coefficients of 20 Classes (6-11 to 10-12)

WALSH 6-11 TO 10-12

F-RATIO VECTOR. NR SIG PER CLASS = 25 NR CLASSES = 20

N	GLOBAL MEAN	F - RATIO	RANK	F - RATIO
1	.421459854	.94382E+03	3	.13845E+05
2	-.276371837	.16822E+02	6	.29463E+04
3	.180234492	.13845E+05	9	.19316E+04
4	.101912975	.12270E+04	25	.14192E+04
5	-.100674778	.93880E+03	21	.13941E+04
6	-.158544034	.29463E+04	4	.12270E+04
7	.052469350	.10585E+04	10	.10815E+04
8	-.022725660	.92342E+03	7	.10585E+04
9	-.014492664	.19316E+04	26	.95740E+03
10	-.028861068	.10815E+04	1	.94382E+03
11	-.045914553	.43280E+03	5	.93880E+03
12	.024911135	.48538E+03	8	.92342E+03
13	-.063686222	.93308E+02	23	.81742E+03
14	-.085314587	.43180E+03	57	.69750E+03
15	.012225481	.12082E+02	24	.67505E+03
16	-.015699737	.52419E+02	58	.54888E+03
17	-.016392939	.49295E+03	17	.49295E+03
18	-.011567336	.24585E+03	12	.48538E+03
19	-.018360678	.40562E+03	27	.44935E+03
20	-.026983093	.43928E+03	20	.43928E+03
21	-.014538482	.13941E+04	11	.43280E+03
22	-.010047775	.25646E+03	14	.43180E+03
23	-.015147123	.81742E+03	19	.40562E+03
24	-.015672214	.67505E+03	28	.38519E+03
25	-.012974054	.14192E+04	53	.37941E+03
26	-.016723357	.95740E+03	56	.37574E+03
27	-.026574213	.44935E+03	30	.34832E+03
28	.008189458	.38519E+03	55	.27556E+03
29	-.034384355	.79027E+02	59	.26150E+03
30	-.046341300	.34832E+03	22	.25646E+03
31	.003344229	.83294E+01	18	.24585E+03

TABLE D3. Feature Selector (F-Ratio) Test on Walsh Coefficients of 20 Classes (6-11 to 10-12)

WALSH 6-11 TO 10-12 (CONT)

32	-.003937508	.72821E+01	60	.23367E+03
33	-.004391285	.94356E+02	49	.21078E+03
34	-.003328099	.55239E+02	62	.20571E+03
35	-.005259098	.11806E+03	39	.16422E+03
36	-.007195756	.40071E+02	51	.16308E+03
37	-.003813875	.15540E+03	37	.15540E+03
38	-.002785032	.89413E+02	52	.13224E+03
39	-.003943803	.16422E+03	54	.13029E+03
40	-.003647456	.11918E+03	40	.11918E+03
41	-.005117728	.49212E+02	35	.11806E+03
42	-.001877687	.87908E+02	33	.94356E+02
43	-.002985545	.53109E+02	13	.93308E+02
44	-.004045820	.31593E+02	38	.89413E+02
45	-.001935357	.32740E+02	42	.87908E+02
46	-.003251178	.55945E+02	29	.79027E+02
47	-.002478158	.51670E+02	50	.72313E+02
48	-.008079369	.16390E+02	46	.55945E+02
49	-.008163791	.21078E+03	34	.55239E+02
50	-.005558838	.72313E+02	43	.53109E+02
51	-.009373251	.16308E+03	16	.52419E+02
52	-.014026146	.13224E+03	47	.51670E+02
53	-.007172187	.37941E+03	41	.49212E+02
54	-.005473697	.13029E+03	36	.40071E+02
55	-.008266874	.27556E+03	61	.36500E+02
56	-.008029046	.37574E+03	45	.32740E+02
57	-.006842365	.69750E+03	44	.31593E+02
58	-.008202417	.54888E+03	2	.16822E+02
59	-.013011700	.26150E+03	48	.16390E+02
60	.004154839	.23367E+03	15	.12082E+02
61	-.017102443	.36500E+02	31	.83294E+01
62	-.023213081	.20571E+03	32	.72821E+01
63	.001648158	.70162E+01	63	.70162E+01

TABLE D3. (continued)

HAAR 6-11 TO 10-12

F-RATIO VECTOR. NR SIG PER CLASS = 25 NR CLASSES = 20

N	GLOBAL MEAN	F - RATIO	RANK	F - RATIO
1	.421459854	.94382E+03	5	.65954E+04
2	-.067979291	.38147E+04	12	.41875E+04
3	.322869420	.11542E+04	2	.38147E+04
4	-.052418254	.51611E+01	25	.29081E+04
5	-.053656437	.65954E+04	6	.29033E+04
6	.206800520	.29033E+04	24	.27113E+04
7	.004212818	.16141E+03	27	.20938E+04
8	-.079145819	.52838E+01	13	.18742E+04
9	.000045885	.30722E+01	10	.18237E+04
10	.001146692	.18237E+04	22	.13999E+04
11	-.025410343	.78754E+03	26	.12637E+04
12	.056869388	.41875E+04	23	.12631E+04
13	.074749634	.18742E+04	21	.11728E+04
14	.006280228	.14284E+03	3	.11542E+04
15	.000043196	.50746E+01	1	.94382E+03
16	-.067468256	.47637E+01	11	.78754E+03
17	-.003099656	.46635E+01	48	.58286E+03
18	.001361913	.59404E+01	47	.56349E+03
19	-.000485979	.71514E+01	50	.54573E+03
20	.003002785	.17618E+03	49	.49981E+03
21	-.004078226	.11728E+04	51	.41726E+03
22	-.012486210	.13999E+04	55	.38915E+03
23	-.003240537	.12631E+04	43	.34455E+03
24	.014016557	.27113E+04	54	.32788E+03
25	.025838614	.29081E+04	44	.31620E+03
26	.029063039	.12637E+04	45	.29903E+03
27	.023341142	.20938E+04	28	.27999E+03
28	.007274061	.27999E+03	46	.23718E+03
29	-.000141846	.11623E+02	52	.22990E+03
30	.000025079	.65944E+01	53	.21122E+03
31	-.000045565	.58745E+01	20	.17618E+03

TABLE D4. Feature Selector (F-Ratio) Test on Haar Coefficients of 20 Classes (6-11 to 10-12)

HAAR 6-11 TO 10-12 (CONT)

32	-.034772977	.44496E+01	7	.16141E+03
33	-.013562107	.46693E+01	14	.14284E+03
34	-.002439418	.39371E+01	56	.14041E+03
35	.000854119	.25150E+01	42	.10548E+03
36	.001427832	.24802E+01	57	.23660E+02
37	.000458961	.48432E+01	41	.20209E+02
38	-.000580903	.37468E+01	29	.11623E+02
39	-.000193610	.23888E+01	58	.95778E+01
40	.000841666	.88559E+01	40	.88559E+01
41	.000527325	.20209E+02	19	.71514E+01
42	-.000041010	.10548E+03	30	.65944E+01
43	-.002936369	.34455E+03	59	.65067E+01
44	-.004171481	.31620E+03	60	.64988E+01
45	-.004217939	.29903E+03	63	.64573E+01
46	-.002539818	.23718E+03	62	.63902E+01
47	.000350902	.56349E+03	61	.63083E+01
48	.003491787	.58286E+03	18	.59404E+01
49	.005964154	.49981E+03	31	.58745E+01
50	.008566041	.54573E+03	8	.52838E+01
51	.010348957	.41726E+03	4	.51611E+01
52	.010499693	.22990E+03	15	.50746E+01
53	.010017596	.21122E+03	37	.48432E+01
54	.009008653	.32788E+03	16	.47637E+01
55	.007324575	.38915E+03	33	.46693E+01
56	.004464616	.14041E+03	17	.46635E+01
57	.000904510	.23660E+02	32	.44496E+01
58	-.000280508	.95778E+01	34	.39371E+01
59	.000021330	.65067E+01	38	.37468E+01
60	.000050633	.64988E+01	9	.30722E+01
61	-.000114483	.63083E+01	35	.25150E+01
62	-.000000069	.63902E+01	36	.24802E+01
63	.000050732	.64573E+01	39	.23888E+01

TABLE D4. (continued)

FOURIER

F-RATIO VECTOR. NR SIG PER CLASS = 25 NR CLASSES = 79

N	GLOBAL MEAN	F - RATIO	RANK	F - RATIO
1	.244011253	.13646E+07	1	.13646E+07
2	.030544873	.11854E+07	2	.11854E+07
3	.007437990	.29563E+06	3	.29563E+06
4	.004120382	.25194E+06	4	.25194E+06
5	.002111879	.63064E+05	5	.63064E+05
6	.000865536	.12963E+05	6	.12963E+05
7	.000385381	.90581E+04	7	.90581E+04
8	.000240613	.29392E+04	8	.29392E+04
9	.000155630	.89223E+03	9	.89223E+03
10	.000096675	.50438E+03	10	.50438E+03
11	.000065638	.24139E+03	11	.24139E+03
12	.000043440	.15983E+03	12	.15983E+03
13	.000030658	.98446E+02	14	.11621E+03
14	.000023340	.11621E+03	13	.98446E+02
15	.000016273	.94626E+02	15	.94626E+02
16	.000012276	.75074E+02	17	.79197E+02
17	.000010168	.79197E+02	16	.75074E+02
18	.000008259	.66924E+02	18	.66924E+02
19	.000006182	.41279E+02	26	.57435E+02
20	.000006026	.50026E+02	24	.51929E+02
21	.000005957	.50573E+02	23	.51833E+02
22	.000004969	.50682E+02	22	.50682E+02
23	.000004456	.51833E+02	21	.50573E+02
24	.000004095	.51929E+02	20	.50026E+02
25	.000003874	.36995E+02	27	.45930E+02
26	.000003587	.57435E+02	30	.42875E+02
27	.000003761	.45930E+02	19	.41279E+02
28	.000003032	.36979E+02	25	.36995E+02
29	.000003664	.27693E+02	28	.36979E+02
30	.000003656	.42875E+02	31	.30794E+02
31	.000003202	.30794E+02	29	.27693E+02

TABLE D5. Feature Selector (F-Ratio) Test on Fourier Magnitude Coefficients of 79 Classes

FOURIER

GLOBAL WEIGHTED SECOND MOMENTS. NR CLASSES = 79

N	GLOBAL MEAN	WTD MOMENT	RANK	WTD MOMENT
1	.244011253	.81307E+05	1	.81307E+05
2	.030544873	.34596E+05	2	.34596E+05
3	.007437990	.33545E+05	3	.33545E+05
4	.004120382	.17185E+05	4	.17185E+05
5	.002111879	.72055E+04	5	.72055E+04
6	.000865536	.49743E+03	6	.49743E+03
7	.000385381	.19427E+03	7	.19427E+03
8	.000240613	.88671E+02	8	.88671E+02
9	.000155630	.51498E+02	9	.51498E+02
10	.000096675	.37999E+02	10	.37999E+02
11	.000065638	.83954E+01	11	.83954E+01
12	.000043440	.57777E+01	12	.57777E+01
13	.000030658	.29259E+01	17	.45425E+01
14	.000023340	.42502E+01	14	.42502E+01
15	.000016273	.32881E+01	15	.32881E+01
16	.000012276	.22817E+01	13	.29259E+01
17	.000010168	.45425E+01	22	.26202E+01
18	.000008259	.18282E+01	16	.22817E+01
19	.000006182	.13818E+01	20	.19179E+01
20	.000006026	.19179E+01	18	.18282E+01
21	.000005957	.14677E+01	26	.18179E+01
22	.000004969	.26202E+01	27	.17297E+01
23	.000004456	.12907E+01	30	.16634E+01
24	.000004095	.15577E+01	25	.16206E+01
25	.000003874	.16206E+01	24	.15577E+01
26	.000003587	.18179E+01	28	.14810E+01
27	.000003761	.17297E+01	31	.14747E+01
28	.000003032	.14810E+01	21	.14677E+01
29	.000003664	.90337E+00	19	.13818E+01
30	.000003656	.16634E+01	23	.12907E+01
31	.000003202	.14747E+01	29	.90337E+00

TABLE D6. Feature Selector (G-Variance Ratio) Test on Fourier Magnitude Coefficients of 79 Classes

WALSH

F-RATIO VECTOR. NR SIG PER CLASS = 25 NR CLASSES = 79

N	GLOBAL MEAN	F - RATIO	RANK	F - RATIO
1	.565311790	.18709E+05	5	.19245E+05
2	-.217285603	.38569E+04	1	.18709E+05
3	.103944555	.11957E+05	4	.18401E+05
4	-.053110689	.18401E+05	29	.12934E+05
5	-.180918634	.19245E+05	3	.11957E+05
6	-.107709035	.23209E+04	28	.11363E+05
7	.030635044	.19884E+04	13	.10376E+05
8	-.040665880	.34298E+04	12	.97208E+04
9	-.044336051	.33474E+04	27	.64322E+04
10	-.022559818	.42024E+04	11	.59864E+04
11	-.029491160	.59864E+04	60	.55136E+04
12	-.042010292	.97208E+04	61	.43864E+04
13	-.102987796	.10376E+05	10	.42024E+04
14	-.069822848	.82600E+03	25	.41552E+04
15	.001940256	.30388E+03	26	.40892E+04
16	-.016583100	.45342E+03	2	.38569E+04
17	-.020561803	.11594E+04	21	.36362E+04
18	-.011698609	.16507E+04	59	.34932E+04
19	-.015326099	.27382E+04	20	.34443E+04
20	-.016030990	.34443E+04	8	.34298E+04
21	-.012256719	.36362E+04	23	.34015E+04
22	-.017078027	.27946E+04	24	.33631E+04
23	-.013291242	.34015E+04	9	.33474E+04
24	-.022318721	.33631E+04	22	.27946E+04
25	-.025561351	.41552E+04	19	.27382E+04
26	-.013324937	.40892E+04	57	.25764E+04
27	-.017566111	.64322E+04	6	.23209E+04
28	-.023117185	.11363E+05	58	.21546E+04
29	-.052535623	.12934E+05	56	.20902E+04
30	-.037340686	.11378E+04	7	.19884E+04
31	-.000379351	.21822E+03	52	.17819E+04

TABLE D7. Feature Selector (F-Ratio) Test on Walsh Coefficients of 79 Classes

WALSH (CONT)

32	-.002763121	.85677E+02	18	.16507E+04
33	-.003858594	.16422E+03	55	.15446E+04
34	-.001771946	.14446E+03	53	.14643E+04
35	-.002504065	.33111E+03	54	.12274E+04
36	-.002813622	.59134E+03	17	.11594E+04
37	-.001669894	.48991E+03	30	.11378E+04
38	-.002616133	.30749E+03	51	.10275E+04
39	-.001990825	.47213E+03	62	.97721E+03
40	-.000862905	.37063E+03	14	.82600E+03
41	-.002232825	.27667E+03	36	.59134E+03
42	-.001120716	.21317E+03	50	.56949E+03
43	-.001534370	.17058E+03	49	.53684E+03
44	-.001099636	.21086E+03	37	.48991E+03
45	-.000131854	.17027E+03	39	.47213E+03
46	-.001377116	.20433E+03	16	.45342E+03
47	-.000502281	.17193E+03	40	.37063E+03
48	-.007560768	.16286E+03	35	.33111E+03
49	-.009521550	.53684E+03	38	.30749E+03
50	-.005135024	.56949E+03	15	.30388E+03
51	-.006912556	.10275E+04	41	.27667E+03
52	-.007238736	.17819E+04	31	.21820E+03
53	-.005216978	.14643E+04	42	.21317E+03
54	-.007828495	.12274E+04	44	.21086E+03
55	-.006029200	.15446E+04	46	.20433E+03
56	-.010537105	.20902E+04	47	.17193E+03
57	-.012210166	.25764E+04	43	.17058E+03
58	-.006000713	.21546E+04	45	.17027E+03
59	-.008100864	.34932E+04	33	.16422E+03
60	-.010843758	.55136E+04	48	.16286E+03
61	-.025686976	.43864E+04	34	.14446E+03
62	-.018169586	.97721E+03	32	.85677E+02
63	.000486727	.60132E+02	63	.60132E+02

TABLE D7. (continued)

WALSH

GLOBAL WEIGHTED SECOND MOMENTS. NR CLASSES = 79

N	GLOBAL MEAN	WTD MOMENT	RANK	WTD MOMENT
1	.565311790	.13590E+04	4	.87650E+04
2	-.217285603	.67881E+02	5	.42234E+04
3	.103944555	.31066E+04	3	.31066E+04
4	-.053110689	.87650E+04	12	.13955E+04
5	-.180918634	.42234E+04	1	.13590E+04
6	-.107709035	.32753E+03	13	.76792E+03
7	.030635044	.27490E+03	10	.62367E+03
8	-.040665880	.45347E+03	28	.50915E+03
9	-.044336051	.28946E+03	11	.47813E+03
10	-.022559818	.62367E+03	8	.45347E+03
11	-.029491160	.47813E+03	29	.34414E+03
12	-.042010292	.13955E+04	6	.32753E+03
13	-.102987796	.76792E+03	9	.28946E+03
14	-.069822848	.35172E+02	7	.27490E+03
15	.001940256	.98932E+01	27	.26488E+03
16	-.016583100	.11939E+02	26	.23225E+03
17	-.020561803	.47388E+02	20	.19803E+03
18	-.011698609	.49247E+02	25	.19704E+03
19	-.015326099	.77826E+02	24	.18797E+03
20	-.016030990	.19803E+03	22	.14856E+03
21	-.012256719	.12389E+03	60	.12543E+03
22	-.017078027	.14856E+03	21	.12389E+03
23	-.013291242	.11665E+03	23	.11665E+03
24	-.022318721	.18797E+03	61	.10899E+03
25	-.025561351	.19704E+03	59	.89312E+02
26	-.013324937	.23225E+03	19	.77826E+02
27	-.017566111	.26488E+03	2	.67881E+02
28	-.023117185	.50915E+03	56	.62724E+02
29	-.052535623	.34414E+03	58	.49439E+02
30	-.037340686	.28778E+02	18	.49247E+02
31	-.000379351	.48499E+01	57	.47756E+02

TABLE D8. Feature Selector (G-Variance Ratio) Test on Walsh Coefficients of 79 Classes

WALSH (CONT)

32	-.002763121	.16543E+01	17	.47388E+02
33	-.003858594	.34326E+01	52	.36842E+02
34	-.001771946	.52938E+01	14	.35172E+02
35	-.002504065	.85940E+01	55	.34456E+02
36	-.002813622	.15359E+02	30	.28778E+02
37	-.001669894	.13186E+02	53	.28266E+02
38	-.002616133	.59670E+01	62	.27122E+02
39	-.001990825	.95801E+01	51	.24274E+02
40	-.000862905	.77226E+01	54	.23803E+02
41	-.002232825	.80924E+01	36	.15359E+02
42	-.001120716	.53087E+01	37	.13186E+02
43	-.001534370	.50344E+01	16	.11939E+02
44	-.001099636	.10175E+02	44	.10175E+02
45	-.000131854	.51846E+01	15	.98932E+01
46	-.001377116	.45302E+01	49	.98725E+01
47	-.000502281	.38544E+01	39	.95801E+01
48	-.007560768	.21936E+01	50	.94851E+01
49	-.009521550	.98725E+01	35	.85940E+01
50	-.005135024	.94851E+01	41	.80924E+01
51	-.006912556	.24274E+02	40	.77226E+01
52	-.007238736	.36842E+02	38	.59670E+01
53	-.005216978	.28266E+02	42	.53087E+01
54	-.007828495	.23803E+02	34	.52938E+01
55	-.006029200	.34456E+02	45	.51846E+01
56	-.010537105	.62724E+02	43	.50344E+01
57	-.012210166	.47756E+02	31	.48499E+01
58	-.006000713	.49439E+02	46	.45302E+01
59	-.008100864	.89312E+02	47	.38544E+01
60	-.010843758	.12543E+03	33	.34326E+01
61	-.025686976	.10899E+03	48	.21936E+01
62	-.018169586	.27122E+02	32	.16543E+01
63	.000486727	.10623E+01	63	.10623E+01

TABLE D8. (continued)

HAAR

F-RATIO VECTOR. NR SIG PER CLASS = 25 NR CLASSES = 79

N	GLOBAL MEAN	F - RATIO	RANK	F - RATIO
1	.565311790	.18709E+05	3	.20366E+05
2	-.080144212	.40094E+04	1	.18709E+05
3	.227144033	.20366E+05	5	.15571E+05
4	-.155551642	.56587E+04	12	.10324E+05
5	.078477696	.15571E+05	6	.10047E+05
6	.133076042	.10047E+05	11	.98117E+04
7	.005268052	.16782E+04	13	.90949E+04
8	-.123720288	.12499E+04	24	.87025E+04
9	-.026809175	.58476E+04	21	.85684E+04
10	.015614549	.84870E+04	10	.84870E+04
11	.038914397	.98117E+04	23	.82532E+04
12	.045777909	.10324E+05	27	.73474E+04
13	.048083924	.90949E+04	25	.66174E+04
14	.007561467	.18583E+04	22	.62710E+04
15	.000065082	.10602E+02	18	.61692E+04
16	-.078742653	.23280E+03	20	.60012E+04
17	-.017329343	.48708E+04	9	.58476E+04
18	-.010028591	.61692E+04	26	.56997E+04
19	-.007272270	.55549E+04	4	.56587E+04
20	.002185489	.60012E+04	19	.55549E+04
21	.008286370	.85684E+04	17	.48708E+04
22	.011720791	.62710E+04	2	.40094E+04
23	.015740100	.82532E+04	43	.31419E+04
24	.016436238	.87025E+04	28	.27804E+04
25	.016254377	.66174E+04	42	.27716E+04
26	.016929265	.56997E+04	45	.26860E+04
27	.016759910	.73474E+04	39	.26273E+04
28	.007548493	.27804E+04	40	.25358E+04
29	-.000035129	.70845E+02	41	.25028E+04
30	.000026063	.13846E+02	44	.24087E+04
31	.000003486	.12519E+02	36	.23791E+04

TABLE D9. Feature Selector (F-Ratio) Test on Haar Coefficients of 79 Classes

HAAR (CONT)

32	-.030998804	.71907E+02	37	.23272E+04
33	-.020798806	.36716E+03	47	.22528E+04
34	-.008263538	.15029E+04	38	.21674E+04
35	-.004329727	.18157E+04	55	.21475E+04
36	-.003420372	.23791E+04	48	.20354E+04
37	-.003714766	.23272E+04	46	.19179E+04
38	-.003357950	.21674E+04	14	.18583E+04
39	-.001785635	.26273E+04	35	.18157E+04
40	.000036728	.25358E+04	7	.16782E+04
41	.001294567	.25028E+04	34	.15029E+04
42	.002697312	.27716E+04	49	.14999E+04
43	.003185426	.31419E+04	54	.14583E+04
44	.003788556	.24087E+04	50	.14412E+04
45	.004647519	.26860E+04	51	.14327E+04
46	.005146206	.19179E+04	56	.12952E+04
47	.005858616	.22528E+04	53	.12796E+04
48	.005964712	.20354E+04	8	.12499E+04
49	.005714301	.14999E+04	52	.11742E+04
50	.005673340	.14412E+04	57	.57037E+03
51	.006033399	.14327E+04	33	.36716E+03
52	.006039556	.11742E+04	16	.23280E+03
53	.006098758	.12796E+04	32	.71907E+02
54	.006267068	.14583E+04	29	.70845E+02
55	.005584360	.21475E+04	58	.62252E+02
56	.003954230	.12952E+04	59	.18718E+02
57	.001400578	.57037E+03	61	.16565E+02
58	-.000000463	.62252E+02	62	.16325E+02
59	.000009989	.18718E+02	30	.13846E+02
60	.000013213	.13684E+02	60	.13684E+02
61	-.000028365	.16565E+02	63	.13495E+02
62	.000021590	.16325E+02	31	.12519E+02
63	.000021762	.13495E+02	15	.10602E+02

TABLE D9. (continued)

HAAR

GLOBAL WEIGHTED SECOND MOMENTS. NR CLASSES = 79

N	GLOBAL MEAN	WTD MOMENT	RANK	WTD MOMENT
1	.565311790	.13590E+04	7	.21813E+37
2	-.080144212	.23700E+03	13	.21813E+37
3	.227144033	.26014E+04	14	.21813E+37
4	-.155551642	.60665E+03	15	.21813E+37
5	.078477696	.52823E+04	26	.21813E+37
6	.133076042	.60607E+03	27	.21813E+37
7	.005268052	.21813E+37	28	.21813E+37
8	-.123720288	.86505E+02	29	.21813E+37
9	-.026809175	.53364E+03	30	.21813E+37
10	.015614549	.82489E+03	31	.21813E+37
11	.038914397	.14071E+04	37	.21813E+37
12	.045777909	.15639E+04	38	.21813E+37
13	.048083924	.21813E+37	39	.21813E+37
14	.007561467	.21813E+37	43	.21813E+37
15	.000065082	.21813E+37	45	.21813E+37
16	-.078742653	.14884E+02	51	.21813E+37
17	-.017329343	.12823E+03	52	.21813E+37
18	-.010028591	.27691E+03	53	.21813E+37
19	-.007272270	.24777E+03	54	.21813E+37
20	.002185489	.17905E+03	55	.21813E+37
21	.008286370	.27031E+03	56	.21813E+37
22	.011720791	.30375E+03	57	.21813E+37
23	.015740100	.33230E+03	58	.21813E+37
24	.016436238	.37681E+03	59	.21813E+37
25	.016254377	.34080E+03	60	.21813E+37
26	.016929265	.21813E+37	61	.21813E+37
27	.016759910	.21813E+37	62	.21813E+37
28	.007548493	.21813E+37	63	.21813E+37
29	-.000035129	.21813E+37	35	.16375E+06
30	.000026063	.21813E+37	36	.37971E+05
31	.000003486	.21813E+37	40	.26643E+05

TABLE D10. Feature Selector (G-Variance Ratio) Test on Haar Coefficients of 79 Classes

HAAR (CONT)

32	-.030998804	.18503E+01	42	.80963E+04
33	-.020798806	.15598E+02	5	.52823E+04
34	-.008263538	.32671E+02	3	.26014E+04
35	-.004329727	.16375E+06	12	.15639E+04
36	-.003420372	.37971E+05	11	.14071E+04
37	-.003714766	.21813E+37	1	.13590E+04
38	-.003357950	.21813E+37	10	.82489E+03
39	-.001785635	.21813E+37	4	.60665E+03
40	.000036728	.26643E+05	6	.60607E+03
41	.001294567	.32313E+02	9	.53364E+03
42	.002697312	.80963E+04	24	.37681E+03
43	.003185426	.21813E+37	25	.34080E+03
44	.003788556	.50924E+02	23	.33230E+03
45	.004647519	.21813E+37	22	.30375E+03
46	.005146206	.45074E+02	18	.27691E+03
47	.005858616	.41865E+02	21	.27031E+03
48	.005964712	.32577E+02	19	.24777E+03
49	.005714301	.31696E+02	2	.23700E+03
50	.005673340	.32009E+02	20	.17905E+03
51	.006033399	.21813E+37	17	.12823E+03
52	.006039556	.21813E+37	8	.86505E+02
53	.006098758	.21813E+37	44	.50924E+02
54	.006267068	.21813E+37	46	.45074E+02
55	.005584360	.21813E+37	47	.41865E+02
56	.003954230	.21813E+37	34	.32671E+02
57	.001400578	.21813E+37	48	.32577E+02
58	-.000000463	.21813E+37	41	.32313E+02
59	.000009989	.21813E+37	50	.32009E+02
60	.000013213	.21813E+37	49	.31696E+02
61	-.000028365	.21813E+37	33	.15598E+02
62	.000021590	.21813E+37	16	.14884E+02
63	.000021762	.21813E+37	32	.18503E+01

TABLE D10. (continued)

LIST OF REFERENCES

1. The Johns Hopkins University Carlyle Barton Laboratory, Technical Report AFAL-TR-70-307, A Comparison of Linear Bases for Pulsed Signals, Bennett, R. S., January 1971.

2. The Johns Hopkins University Carlyle Barton Laboratory, Technical Report AFAL-TR-70-89, A Nonlinear Representation for Parametrically Similar Signals, Bennett, R. S., May 1970.

3. Andrews, H. C., Computer Techniques in Image Processing, Academic Press, 1970.

4. Andrews, H. C., Mathematical Techniques in Pattern Recognition, John Wiley, 1972.

5. Terman, F. E., Radio Engineering, Third Ed., McGraw-Hill, 1947, p. 786-789.

6. Fino, B. J., "Relations Between Haar and Walsh/Hadamard Transforms," Proceedings of the IEEE, v. 60, p. 647, 648, May 1972.

7. Fu, K. S., Min, P. J., Li, T. J., "Feature Selection in Pattern Recognition," IEEE Transactions on Systems Science and Cybernetics, v. 6, p. 33-39, January 1970.

8. Michael, M. T., Lin, W-C., "Experimental Study of Information Measure and Inter-Intra Class Distance Ratios on Feature Selection and Orderings," IEEE Transactions on Systems, Man, and Cybernetics, v. 3, p. 172-181, March 1973.

9. Sebestyen, G. S., Decision Making Processes in Pattern Recognition, p. 17-23, 25-30, MacMillan, 1962.

10. Moroney, M. J., Facts From Figures, p. 334-370, Penguin Books Ltd, 1951.

11. Fowle, F. F., "The Transposition of Conductors," Transactions AIEE, v. 23, p. 659-687, 1905.

12. Walsh, J. L., "A Closed Set of Normal Orthogonal Functions," American Journal of Mathematics, v. 45, p. 5-24, 1923.

13. Rademacher, H., "Einige Satze uber Reihen von allegemeinen Orthogonalfunktionen," Math. Annalen, v. 87, p. 112-138, 1922.

14. Harmuth, H. F., Transmission of Information by Orthogonal Functions, Springler-Verlag, Berlin/New York, 1969.

15. Haar, A., "Zur Theorie der Orthogonalen Funktionensysteme," Math Annalen, v. 69, p. 331-371, 1910.

16. Swick, D. A., "Walsh Function Generation," IEEE Transactions on Information Theory, v. IT-15, p. 167, January 1969.

17. Peterson, H. L., "Generation of Walsh Functions," Symposium on Walsh Functions, Naval Research Lab., Washington, D.C., 1970.

18. Robinson, G. S., "Discrete Walsh Functions and Their Applications," COMSAT Laboratories, Clarksburg, Md., 1970.

19. Shore, J. E., "On the Application of Haar Functions," IEEE Transactions on Communications, v. COM-21, p. 209-216, March 1973.

20. Rejchrt, V. J., "Signal Flow Graph and a Fortran Program for the Haar-Fourier Transform," IEEE Transactions on Computers, v. C-21, p. 1026-1027, September 1972.

INITIAL DISTRIBUTION LIST

		No. Copies
1.	Defense Documentation Center Cameron Station Alexandria, Virginia 22314	2
2.	Library, Code 0212 Naval Postgraduate School Monterey, California 93940	2
3.	Assoc. Professor Stephen Jauregui, Jr. Code 52Ja Department of Electrical Engineering Naval Postgraduate School Monterey, California 93940	10
4.	LT John D. Meloy USN NAVSECGRU HQ, G-83 3801 Nebraska Ave., N.W. Washington, D.C. 20390	1
5.	Assistant Secretary of Defense for Intelligence The Pentagon Washington, D.C. 20350 ATTN: CDR J.W.R. Pope	1
6.	National Security Agency W Group Fort. G.G. Meade, Maryland 20755 ATTN: James Boone	1
7.	Naval Security Group Headquarters 3801 Nebraska Avenue, N.W. Washington, D.C. 20390 ATTN: CDR H. Orejuela	1
8.	Naval Electronic Systems Command PME 107 Washington, D.C. 20360 ATTN: R. Shields	1

REPORT DOCUMENTATION PAGE

READ INSTRUCTIONS BEFORE COMPLETING FORM

1. REPORT NUMBER	2. GOVT ACCESSION NO.	3. RECIPIENT'S CATALOG NUMBER
4. TITLE (and Subtitle) The Feasibility of Pulse Signal Classification by Spectral Parameters		5. TYPE OF REPORT & PERIOD COVERED Engineer's Thesis; December 1973
		6. PERFORMING ORG. REPORT NUMBER
7. AUTHOR(s) John Donald Meloy		8. CONTRACT OR GRANT NUMBER(s)
9. PERFORMING ORGANIZATION NAME AND ADDRESS Naval Postgraduate School Monterey, California 93940		10. PROGRAM ELEMENT, PROJECT, TASK AREA & WORK UNIT NUMBERS
11. CONTROLLING OFFICE NAME AND ADDRESS Naval Postgraduate School Monterey, California 93940		12. REPORT DATE December 1973
		13. NUMBER OF PAGES 98
14. MONITORING AGENCY NAME & ADDRESS(if different from Controlling Office) Naval Postgraduate School Monterey, California 93940		15. SECURITY CLASS. (of this report) Unclassified
		15a. DECLASSIFICATION/DOWNGRADING SCHEDULE

16. DISTRIBUTION STATEMENT (of this Report)

Approved for public release; distribution unlimited.

17. DISTRIBUTION STATEMENT (of the abstract entered in Block 20, if different from Report)

18. SUPPLEMENTARY NOTES

19. KEY WORDS (Continue on reverse side if necessary and identify by block number)

Pulse Classification
Radar Classification
Signal Classification
Dimensionality Reduction
Signal Transforms

20. ABSTRACT (Continue on reverse side if necessary and identify by block number)

This paper explores the feasibility of fast transform coefficients as classification features for pulse type signals. The fast transforms investigated are Fourier (FFT), Walsh (FWT), and Haar (FHT). A synthesized signal base containing 79 distinct pulse shapes of similar duration is analyzed for classification information compactness in the discrete time, Fourier, Walsh, and Haar bases. Non-parametric information measures are used. It is

(20.) concluded that a Fourier basis representation enables the significant reduction of dimensionality necessary for further study as a generator of classification features.

Thesis
M4498
c.1
147981
Meloy
The feasibility of
pulse signal classification by special
parameters.